JACS
JOURNAL OF THE AMERICAN CHEMICAL SOCIETY
Article
pubs.acs.org/JACS

A New Class of Transition Metal Pincer Ligand: Tantalum Complexes that Feature a [*CCC*] X_3-Donor Array Derived from a Terphenyl Ligand

Aaron Sattler and Gerard Parkin*

Department of Chemistry, Columbia University, New York, New York 10027, United States

Supporting Information

ABSTRACT: A new class of [*CCC*] X_3-donor pincer ligand for transition metals has been constructed *via* cyclometalation of a 2,6-di-*p*-tolylphenyl ([Ar^{Tol_2}]) derivative. Specifically, addition of PMe_3 to [Ar^{Tol_2}]$TaMe_3Cl$ induces elimination of methane and formation of the pincer complex, [κ^3-$Ar^{Tol'_2}$]-$Ta(PMe_3)_2MeCl$ (Tol′ = C_6H_3Me), which may also be obtained by treatment of $Ta(PMe_3)_2Me_3Cl_2$ with [Ar^{Tol_2}]Li. Solutions of [κ^3-$Ar^{Tol'_2}$]$Ta(PMe_3)_2MeCl$ undergo ligand redistribution with the formation of [κ^3-$Ar^{Tol'_2}$]$Ta(PMe_3)_2Me_2$ and [κ^3-$Ar^{Tol'_2}$]$Ta(PMe_3)_2Cl_2$, which may also be synthesized by the reactions of [κ^3-$Ar^{Tol'_2}$]$Ta(PMe_3)_2MeCl$ with MeMgBr and $ZnCl_2$, respectively. Reduction of [κ^3-$Ar^{Tol'_2}$]$Ta(PMe_3)_2Cl_2$ with KC_8 in benzene gives the benzene complex [κ^3-$Ar^{Tol'_2}$]-$Ta(PMe_3)_2(\eta^6$-$C_6H_6)$ that is better described as a 1,4-cyclohexadienediyl derivative. Deuterium labeling employing $Ta(PMe_3)_2$-$(CD_3)_3Cl_2$ demonstrates that the pincer ligand is created by a pair of Ar−H/Ta−Me sigma-bond metathesis transformations, rather than by a mechanism that involves α-H abstraction by a tantalum methyl ligand.

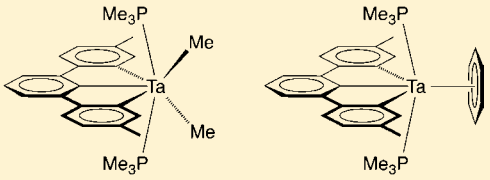

INTRODUCTION

So-called "pincer" ligands, which bind to a metal with a κ^3-tridentate meridional (*i.e.*, "T"-shaped) motif (Figure 1), are an important class of ligands that have received much attention in areas as diverse as (i) fundamental chemical transformations involving bond activation, (ii) catalysis, (iii) sensors, (iv) switches, and (v) supramolecular chemistry.[1] A large array of such ligands are known, and, in many cases, the backbone features six-membered aromatic rings that either contain the central **A** donor (Figure 1, II) or serve as a linker to the lateral **B** donors (Figure 1, III). Such an arrangement enforces planarity with respect to the coordination sphere, especially when the donors are located in such a manner as to form two five-membered chelate rings. One of the reasons for the widespread applications of pincer ligands is that it is possible to vary the nature of the donors in significant ways, thereby providing an effective means to modulate the properties of a metal center.

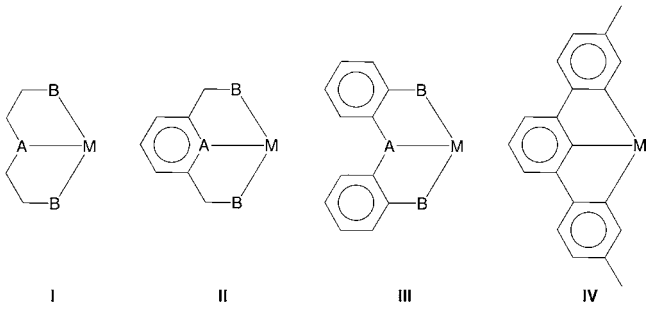

Figure 1. Pincer ligand motifs.

For example, pincer ligands are known for each of the L_3, L_2X, LX_2, and X_3 Covalent Bond Classifications,[2] which provides a clear indication of the electronic variations that may be achieved within this system of ligands.[1] Furthermore, pincer ligands may incorporate a variety of donor atoms, of which [*NCN*] and [*PCP*] are common examples.[1] Notably absent from the large collection of known pincer ligands for transition metals, however, are those that feature a planar [*CCC*] X_3-donor array,[3−5] an observation that may reflect synthetic difficulties. Therefore, it is significant that we introduce here a [*CCC*] X_3-donor pincer ligand and describe its application to tantalum chemistry.

RESULTS AND DISCUSSION

1. Synthesis and Structural Characterization of Tantalum Complexes That Feature a [*CCC*] X_3-Donor Pincer Ligand. We rationalized that access to an X_3-donor [*CCC*] pincer ligand (Figure 1, IV) could be achieved by cyclometalation[6,7] of a terphenyl derivative. For this purpose, the *p*-tolyl variant, namely 2,6-di-*p*-tolylphenyl ([Ar^{Tol_2}]), was selected in view of the spectroscopic handle that is provided by the methyl groups. The lithium derivative [Ar^{Tol_2}]Li is conveniently obtained from [Ar^{Tol_2}]I[8] by treatment with Bu^nLi, from which [Ar^{Tol_2}]$TaMe_3Cl$ can be obtained *via* reaction with $TaMe_3Cl_2$[9] (Scheme 1). [Ar^{Tol_2}]$TaMe_3Cl$ exhibits limited stability in solution and converts to, *inter alia*, [Ar^{Tol_2}]-$TaMe_2Cl_2$.

The molecular structures of both [Ar^{Tol_2}]$TaMe_3Cl$ and [Ar^{Tol_2}]$TaMe_2Cl_2$ have been determined by X-ray diffraction

Received: November 4, 2011
Published: January 19, 2012

dx.doi.org/10.1021/ja210404x | *J. Am. Chem.Soc.* 2012, 134, 2355−2366

Scheme 1

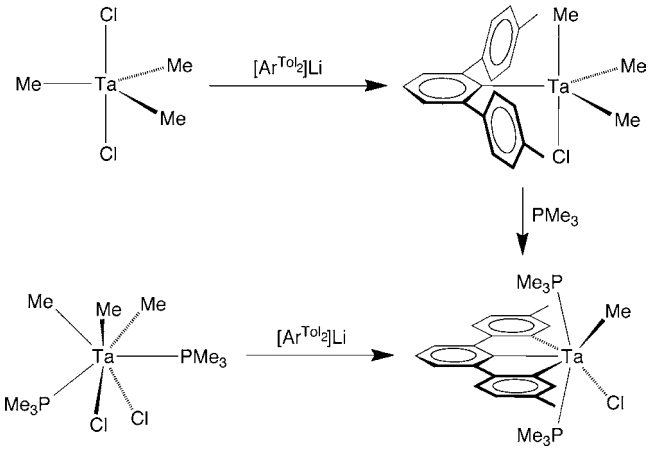

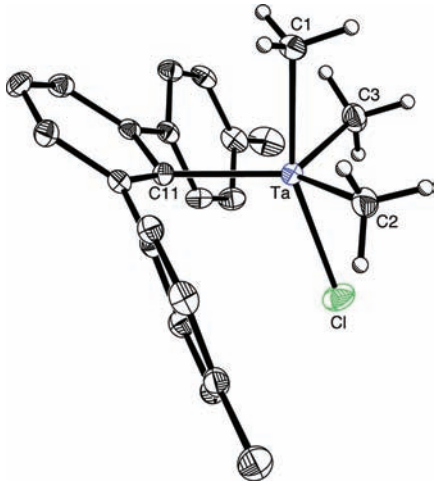

Figure 2. Molecular structure of $[Ar^{Tol_2}]TaMe_3Cl$. Selected bond lengths (Å): Ta–C(11) 2.116(3), Ta–C(1) 2.190(4), Ta–C(2) 2.134(4), Ta–C(3) 2.150(4), Ta–Cl 2.376(1).

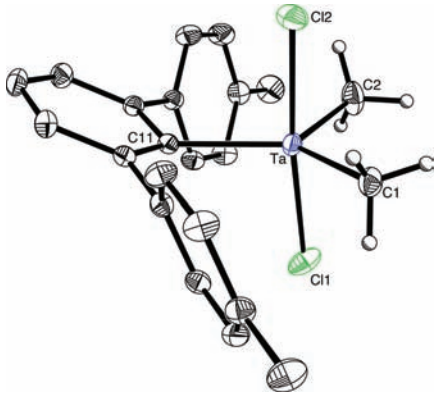

Figure 3. Molecular structure of $[Ar^{Tol_2}]TaMe_2Cl_2$. Selected bond lengths (Å): Ta–C(11) 2.139(2), Ta–C(1) 2.129(2), Ta–C(2) 2.130(3), Ta–Cl(1) 2.313(1), Ta–Cl(2) 2.329(1).

(Figures 2 and 3, respectively), thereby demonstrating that while $[Ar^{Tol_2}]TaMe_2Cl_2$ is an approximate trigonal bipyramid (with axial Cl substituents), the structure of $[Ar^{Tol_2}]TaMe_3Cl$ is distorted towards a square pyramidal geometry. The most interesting feature of the structures of $[Ar^{Tol_2}]TaMe_3Cl$ and $[Ar^{Tol_2}]TaMe_2Cl_2$, however, pertains to the fact that the tantalum atom in each of these complexes is displaced substantially from the plane of the aryl ligand.[10] Specifically, the Ta–C_{ipso}–C_{para} angles in $[Ar^{Tol_2}]TaMe_3Cl$ (145.1°) and $[Ar^{Tol_2}]TaMe_2Cl_2$ (157.1°) deviate considerably from 180°, as illustrated by the views in Figures 2 and 3.

Since tantalum phenyl compounds do not exhibit distortions of this magnitude,[11,12] the unusual displacement of tantalum from the respective aryl planes in $[Ar^{Tol_2}]TaMe_3Cl$ and $[Ar^{Tol_2}]TaMe_2Cl_2$ may be attributed to increased steric interactions between the tolyl groups and the equatorial methyl substituents that would result if the tantalum were to reside in the aryl plane. In support of this notion, density functional theory geometry optimization calculations on the phenyl counterparts, $PhTaMe_3Cl$ and $PhTaMe_2Cl_2$, predict structures in which the tantalum lies in the aryl planes (Figure 4), with

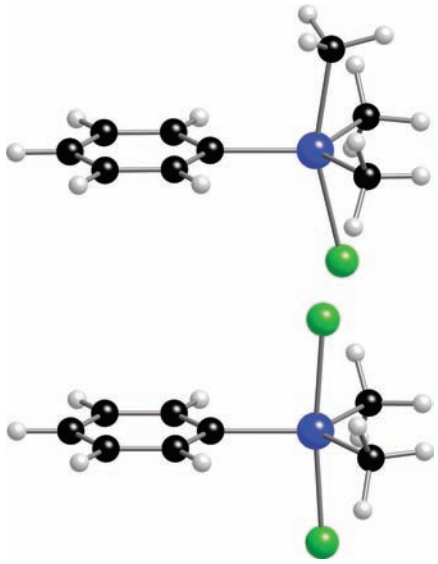

Figure 4. Geometry-optimized structures of $PhTaMe_3Cl$ (top) and $PhTaMe_2Cl_2$ (bottom).

Ta–C_{ipso}–C_{para} angles of 179.4° and 179.9°, respectively, whereas nonplanar geometries that are in accord with the experimental structures are predicted for $[Ar^{Tol_2}]TaMe_3Cl$ (153.3°) and $[Ar^{Tol_2}]TaMe_2Cl_2$ (157.2°); see Supporting Information. Furthermore, the geometry-optimized structure of $PhTaMe_3Cl$ reproduces the distortion towards a square pyramidal geometry that is observed for $[Ar^{Tol_2}]TaMe_3Cl$, thereby suggesting that the square pyramidal distortion is not due to steric factors.

It is also pertinent to note that κ^1-terphenyl compounds do not typically exhibit a displacement of the metal from the aryl plane.[13] For example, the Yb–C_{ipso}–C_{para} angles in five-coordinate $[Ar^{Nap_2}]Yb(THF)_2Cl_2$ and $[Ar^{Mes_2}]Yb(THF)_2Cl_2$ are 180.0° and 172.4°, respectively.[14,15] Likewise, six-coordinate $[Ar^{Mes_2}]Yb(THF)_3Cl_2$ exhibits a normal coordination mode with a Yb–C_{ipso}–C_{para} angle of 176.3°.[15] Distortions of the type observed for $[Ar^{Tol_2}]TaMe_3Cl$ and $[Ar^{Tol_2}]TaMe_2Cl_2$ have, nevertheless, been observed in compounds that feature *two* terphenyl ligands, as illustrated by $[Ar^{Ph_2}]_2Yb(THF)_2$, which has Yb–C_{ipso}–C_{para} angles of 147.6° and 161.9°,[16] and $[Ar^{Ph_2}]_2Eu(THF)_2$, which has Eu–C_{ipso}–C_{para} angles of 145.4° and 159.9°.[17,18]

Of most interest, addition of PMe_3 to $[Ar^{Tol_2}]TaMe_3Cl$ induces elimination of methane and formation of the [CCC]

dx.doi.org/10.1021/ja210404x | J. Am. Chem.Soc. 2012, 134, 2355–2366

pincer complex $[\kappa^3\text{-Ar}^{\text{Tol}'_2}]\text{Ta(PMe}_3)_2\text{MeCl}$ (Tol′ = C_6H_3Me), as illustrated in Scheme 1.[19,20] In this regard, the ability of PMe_3 to induce alkane elimination in Ta(V) compounds by α-H elimination has been previously noted.[21] Alternatively, $[\kappa^3\text{-Ar}^{\text{Tol}'_2}]\text{Ta(PMe}_3)_2\text{MeCl}$ can be obtained directly by treatment of the trimethylphosphine adduct $\text{Ta(PMe}_3)_2\text{Me}_3\text{Cl}_2$[22] with $[\text{Ar}^{\text{Tol}_2}]\text{Li}$. Solutions of $[\kappa^3\text{-Ar}^{\text{Tol}'_2}]\text{Ta(PMe}_3)_2\text{MeCl}$, however, undergo ligand redistribution with the formation of $[\kappa^3\text{-Ar}^{\text{Tol}'_2}]\text{Ta(PMe}_3)_2\text{Me}_2$ and $[\kappa^3\text{-Ar}^{\text{Tol}'_2}]\text{Ta(PMe}_3)_2\text{Cl}_2$, which may also be synthesized by the reactions of $[\kappa^3\text{-Ar}^{\text{Tol}'_2}]\text{Ta(PMe}_3)_2\text{MeCl}$ with MeMgBr and $ZnCl_2$, respectively (Scheme 2).

Scheme 2

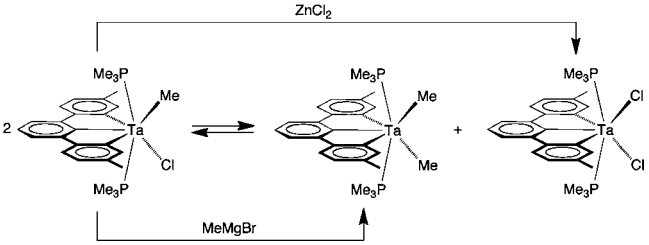

The molecular structures of $[\kappa^3\text{-Ar}^{\text{Tol}'_2}]\text{Ta(PMe}_3)_2\text{Me}_2$, $[\kappa^3\text{-Ar}^{\text{Tol}'_2}]\text{Ta(PMe}_3)_2\text{MeCl}$, and $[\kappa^3\text{-Ar}^{\text{Tol}'_2}]\text{Ta(PMe}_3)_2\text{Cl}_2$ have been determined by X-ray diffraction and confirm the κ^3-planar binding mode of the pincer ligand, as illustrated in Figures 5–7, respectively. The two PMe_3 ligands bind in such a manner that the P–Ta–P plane is approximately orthogonal to the plane of the pincer ligand, while the methyl and chloride ligands are oriented such that the X–Ta–Y plane (X = Me, Cl; Y = Me, Cl) approximately bisects the P–Ta–P and pincer planes. As such, $[\kappa^3\text{-Ar}^{\text{Tol}'_2}]\text{Ta(PMe}_3)_2\text{Me}_2$ and $[\kappa^3\text{-Ar}^{\text{Tol}'_2}]\text{Ta(PMe}_3)_2\text{Cl}_2$ possess molecular C_2 symmetry.

With respect to the binding of the pincer ligand, the three Ta–Ar bond lengths in each complex are very similar (Table 1) and are comparable to the Ta–$[\text{Ar}^{\text{Tol}_2}]$ bond lengths in both $[\text{Ar}^{\text{Tol}_2}]\text{TaMe}_3\text{Cl}$ and $[\text{Ar}^{\text{Tol}_2}]\text{TaMe}_2\text{Cl}_2$. Furthermore, these values are comparable to the mean bond length of 2.23 Å for structurally characterized tantalum phenyl compounds listed in the Cambridge Structural Database.[11] In view of the similarity

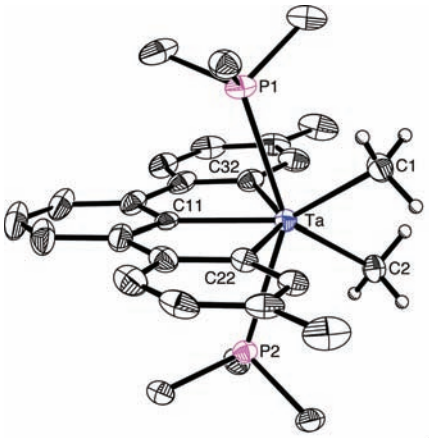

Figure 5. Molecular structure of $[\kappa^3\text{-Ar}^{\text{Tol}'_2}]\text{Ta(PMe}_3)_2\text{Me}_2$. Selected bond lengths (Å): Ta–C(11) 2.200(5), Ta–C(22) 2.243(5), Ta–C(32) 2.230(5), Ta–C(1) 2.212(5), Ta–C(2) 2.211(4), Ta–P(1) 2.631(1), Ta–P(2) 2.622(1).

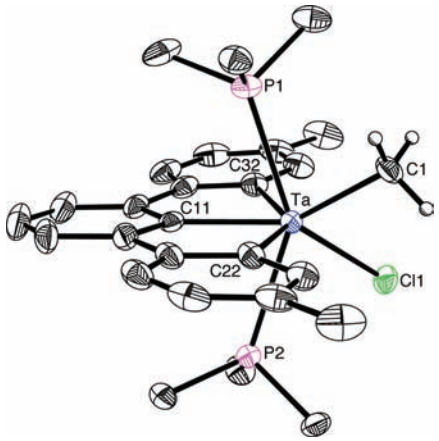

Figure 6. Molecular structure of $[\kappa^3\text{-Ar}^{\text{Tol}'_2}]\text{Ta(PMe}_3)_2\text{MeCl}$ (disorder between Me and Cl not shown). Selected bond lengths (Å): Ta–C(11) 2.190(3), Ta–C(22) 2.230(3), Ta–C(32) 2.227(3), Ta–C(1) 2.18(1) [2.18(1) disordered component], Ta–Cl(1) 2.441(2) [2.484(3) disordered component], Ta–P(1) 2.629(1), Ta–P(2) 2.627(1).

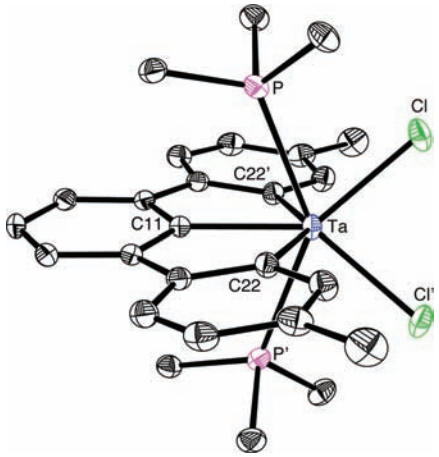

Figure 7. Molecular structure of $[\kappa^3\text{-Ar}^{\text{Tol}'_2}]\text{Ta(PMe}_3)_2\text{Cl}_2$. Selected bond lengths (Å): Ta–C(11) 2.227(4), Ta–C(22) 2.207(3), Ta–Cl 2.4069(7), Ta–P 2.6443(8).

Table 1. Ta–C Bond Lengths Pertaining to Coordination of $[\text{Ar}^{\text{Tol}_2}]$ and $[\kappa^3\text{-Ar}^{\text{Tol}'_2}]$ Ligands[a]

	Ta–C_{cent}/Å	Ta–$C_{lat\#1}$/Å	Ta–$C_{lat\#2}$/Å
$[\kappa^3\text{-Ar}^{\text{Tol}'_2}]\text{Ta(PMe}_3)_2\text{Me}_2$	2.200(5)	2.230(5)	2.243(5)
$[\kappa^3\text{-Ar}^{\text{Tol}'_2}]\text{Ta(PMe}_3)_2\text{Cl}_2$	2.227(4)	2.207(3)	2.207(3)
$[\kappa^3\text{-Ar}^{\text{Tol}'_2}]\text{Ta(PMe}_3)_2\text{MeCl}$	2.190(3)	2.230(3)	2.227(3)
$[\kappa^3\text{-Ar}^{\text{Tol}'_2}]\text{Ta(PMe}_3)_2(\eta^6\text{-C}_6\text{H}_6)$	2.243(2)	2.356(2)	2.362(2)
$[\text{Ar}^{\text{Tol}_2}]\text{TaMe}_3\text{Cl}$	2.116(3)	–	–
$[\text{Ar}^{\text{Tol}_2}]\text{TaMe}_2\text{Cl}_2$	2.139(2)	–	–

[a] cent = central carbon, lat = lateral carbon.

in bond lengths, it would appear that there is little strain associated with the κ^3-coordination mode, a notion that is endorsed by the fact that the Ta–C–C angles in the pincer complexes are also close to the idealized value of 120°.

In addition to the synthesis of methyl and chloride derivatives, the $[\kappa^3\text{-Ar}^{\text{Tol}'_2}]$ pincer ligand also permits isolation of the tantalum benzene complex $[\kappa^3\text{-Ar}^{\text{Tol}'_2}]\text{Ta(PMe}_3)_2(\eta^6\text{-C}_6\text{H}_6)$. Specifically, $[\kappa^3\text{-Ar}^{\text{Tol}'_2}]\text{Ta(PMe}_3)_2(\eta^6\text{-C}_6\text{H}_6)$ may be synthesized by

dx.doi.org/10.1021/ja210404x | J. Am. Chem.Soc. 2012, 134, 2355–2366

Scheme 3

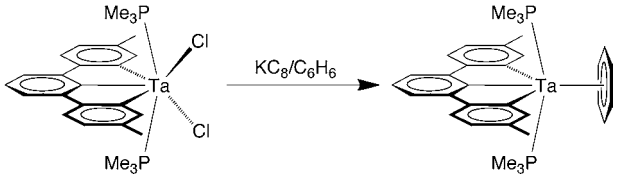

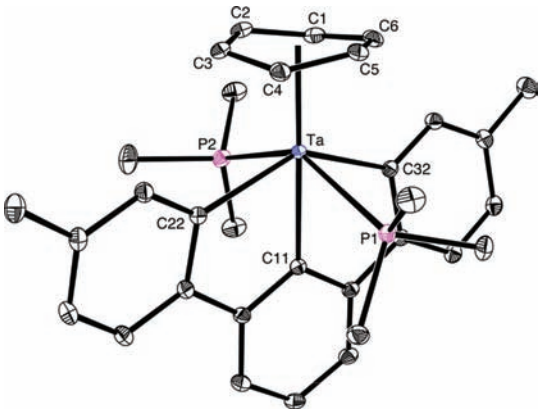

Figure 8. Molecular structure of $[\kappa^3\text{-Ar}^{\text{Tol}'_2}]\text{Ta}(\text{PMe}_3)_2(\eta^6\text{-C}_6\text{H}_6)$. Selected bond lengths (Å): Ta–C(11) 2.243(2), Ta–C(22) 2.356(2), Ta–C(32) 2.362(2), Ta–C(1) 2.316(2), Ta–C(2) 2.478(2), Ta–C(3) 2.431(2), Ta–C(4) 2.317(2), Ta–C(5) 2.496(2), Ta–C(6) 2.439(2), Ta–P(1) 2.6399(8), Ta–P(2) 2.6416(9).

reduction of $[\kappa^3\text{-Ar}^{\text{Tol}'_2}]\text{Ta}(\text{PMe}_3)_2\text{Cl}_2$ with KC_8 in benzene (Scheme 3) and has been structurally characterized by X-ray diffraction, as shown in Figure 8. Interestingly, despite the fact that the first tantalum benzene complex, $\text{Ta}(\eta^6\text{-C}_6\text{H}_6)_2$, was reported in 1981,[23a,b] and a variety of other tantalum arene compounds have also been synthesized,[23c,d] there are no structurally characterized tantalum benzene complexes listed in the Cambridge Structural Database.[11,24] It is, therefore, significant that the molecular structure of $[\kappa^3\text{-Ar}^{\text{Tol}'_2}]\text{Ta}(\text{PMe}_3)_2(\eta^6\text{-C}_6\text{H}_6)$ has been determined by X-ray diffraction. In this regard, a notable feature of $[\kappa^3\text{-Ar}^{\text{Tol}'_2}]\text{Ta}(\text{PMe}_3)_2(\eta^6\text{-C}_6\text{H}_6)$ is that the $\eta^6\text{-C}_6\text{H}_6$ ligand does not coordinate in a planar symmetric manner but is puckered, with a fold angle of 17.1° at C1···C4, such that two of the Ta–C bonds [Ta–C(1) = 2.317(2) Å and Ta–C(4) = 2.318(2) Å] are 0.15 Å shorter than the average for the other four carbon atoms (2.463 Å).[25] Furthermore, the C–C bond lengths of the benzene ring vary, with C(2)–C(3) and C(5)–C(6) (average of 1.373 Å) being significantly shorter than the bonds to C(1) and C(4) (average of 1.436 Å). The localization of the single and double bonds, together with the variation of the Ta–C bond lengths, suggests that the benzene is better described as an L_2X_2 1,4-cyclohexadienediyl ligand (Figure 9).[2,26,27] As such, $[\kappa^3\text{-Ar}^{\text{Tol}'_2}]\text{Ta}(\text{PMe}_3)_2(\eta^6\text{-C}_6\text{H}_6)$ is better classified as a d^0 ML_4X_5 complex, rather than as a d^2 ML_5X_3 derivative.

In accord with the formulation as a d^0 1,4-cyclohexadienediyl derivative, analysis of the Fenske–Hall molecular orbitals[28] indicates that the HOMO of $[\kappa^3\text{-Ar}^{\text{Tol}'_2}]\text{Ta}(\text{PMe}_3)_2(\eta^6\text{-C}_6\text{H}_6)$ is a Ta–$(\eta^6\text{-C}_6\text{H}_6)$ bonding orbital, rather than a metal-based nonbonding orbital that is required for a d^2 description. Specifically, as illustrated in Figure 10, the HOMO represents a

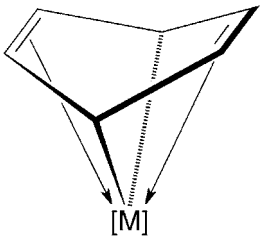

Figure 9. The L_2X_2 1,4-cyclohexadienediyl ligand.

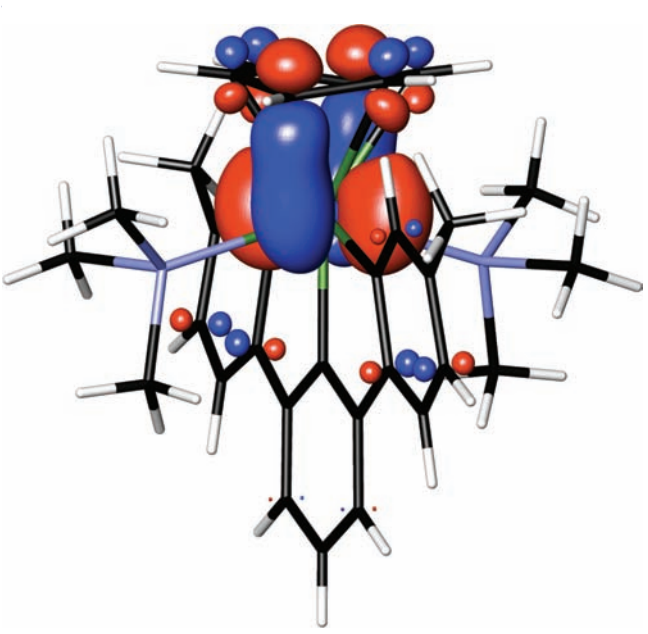

Figure 10. HOMO of $[\kappa^3\text{-Ar}^{\text{Tol}'_2}]\text{Ta}(\text{PMe}_3)_2(\eta^6\text{-C}_6\text{H}_6)$.

δ-interaction between a tantalum d_{xy} orbital[29] and one component of the benzene LUMO e_{2u} set.

2. NMR Spectroscopic Properties of $[\kappa^3\text{-Ar}^{\text{Tol}'_2}]\text{Ta}(\text{PMe}_3)_2\text{Me}_2$. The NMR spectroscopic properties of the dimethyl complex $[\kappa^3\text{-Ar}^{\text{Tol}'_2}]\text{Ta}(\text{PMe}_3)_2\text{Me}_2$ are particularly interesting. For example, while the $^{31}\text{P}\{^1\text{H}\}$ NMR spectrum of $[\kappa^3\text{-Ar}^{\text{Tol}'_2}]\text{Ta}(\text{PMe}_3)_2\text{Me}_2$ is a singlet, indicative of chemically equivalent PMe_3 ligands, the $^{13}\text{C}\{^1\text{H}\}$ NMR signal for the PMe_3 ligands has the appearance of an approximate doublet of triplets (Figure 11), rather than either a doublet (as observed for $[\kappa^3\text{-Ar}^{\text{Tol}'_2}]\text{Ta}(\text{PMe}_3)_2\text{Cl}_2$, *vide infra*) or a virtual triplet.[30] In addition, the $^{13}\text{C}\{^1\text{H}\}$ NMR signal of the tantalum methyl groups does not appear as either a binomial 1:2:1 triplet or a doublet of doublets due to coupling to the two phosphorus nuclei, but rather appears as a non-binomial triplet with an intensity ratio of 1:13.7:1 (Figure 12, left). On the other hand, the corresponding $^{13}\text{C}\{^1\text{H}\}$ NMR signal for the isotopically enriched isotopologue $[\kappa^3\text{-Ar}^{\text{Tol}'_2}]\text{Ta}(\text{PMe}_3)_2(^{13}\text{CH}_3)_2$ exhibits an irregular five-line pattern (Figure 12, right), as does the $^{31}\text{P}\{^1\text{H}\}$ NMR spectrum of $[\kappa^3\text{-Ar}^{\text{Tol}'_2}]\text{Ta}(\text{PMe}_3)_2(^{13}\text{CH}_3)_2$ (Figure 13, right).[31]

The various spectra have been analyzed in detail, and the unusual features of the tantalum methyl region of the $^{13}\text{C}\{^1\text{H}\}$ NMR spectrum are associated with the fact that the two $^2J_{\text{PC}}$ coupling constants have an equal magnitude but are of opposite sign. In this regard, the tantalum methyl groups of natural abundance $[\kappa^3\text{-Ar}^{\text{Tol}'_2}]\text{Ta}(\text{PMe}_3)_2\text{Me}_2$ are a component of an

dx.doi.org/10.1021/ja210404x | J. Am. Chem.Soc. 2012, 134, 2355–2366

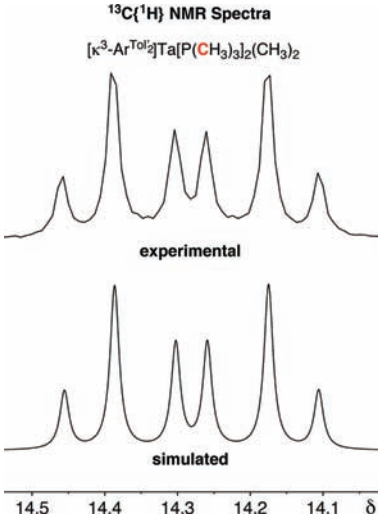

Figure 11. $^{13}C\{^1H\}$ NMR signal for the PMe_3 ligands of $[\kappa^3\text{-}Ar^{Tol'_2}]\text{-}Ta(PMe_3)_2Me_2$.

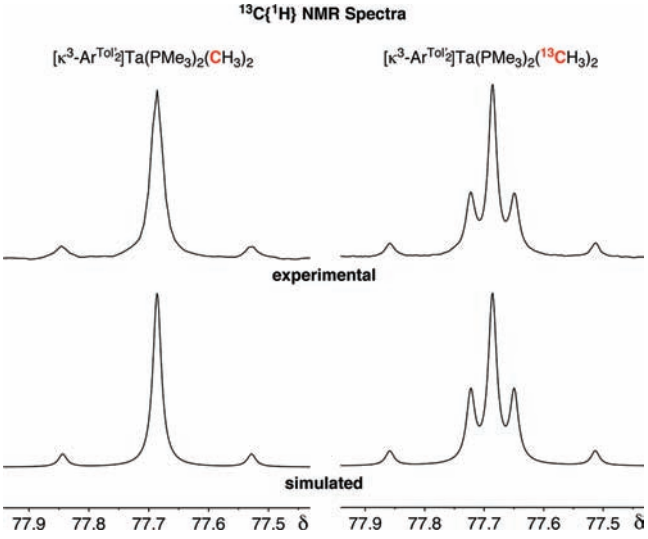

Figure 12. $^{13}C\{^1H\}$ NMR signals for the tantalum methyl ligands of natural abundance $[\kappa^3\text{-}Ar^{Tol'_2}]Ta(PMe_3)_2Me_2$ (left) and ^{13}C-labeled $[\kappa^3\text{-}Ar^{Tol'_2}]\text{-}Ta(PMe_3)_2(^{13}CH_3)_2$ (right).

AA′X spin system (where A = phosphorus and X = carbon), such that the $^{13}C\{^1H\}$ NMR spectrum would be composed of a maximum of five lines.[32,33] The overall appearance of the AA′X spectrum, however, depends on the values of J_{AX}, $J_{A'X}$, and $J_{AA'}$. For example, it is well established that such spectra have a first-order appearance (*i.e.*, a 1:2:1 virtual triplet for X) if $|J_{AA'}| \gg |J_{AX}|, |J_{A'X}|$; under such conditions the line spacing is the average coupling constant, *i.e.*, $^1/_2(J_{AX} + J_{A'X})$. The observation of a triplet does not, however, require that $|J_{AA'}|$ is significantly larger than $|J_{AX}|$ and $|J_{A'X}|$. Specifically, a triplet may also be observed if $J_{AX} = -J_{A'X}$, regardless of the magnitude of $|J_{AA'}|$. However, for such a situation, the intensity ratio of the triplet is not 1:2:1, and the line spacing does not correspond to a single coupling constant but is rather $[(J_{AA'}^2 + J_{AX}^2)]^{1/2}$.[32] Thus, the observation of a non-binomial triplet for the tantalum methyl groups in the $^{13}C\{^1H\}$ NMR spectrum of natural abundance $[\kappa^3\text{-}Ar^{Tol'_2}]\text{-}Ta(PMe_3)_2Me_2$ (Figure 12, upper left) is a consequence of the two $^2J_{PC}$ coupling constants having equal, but opposite, values,

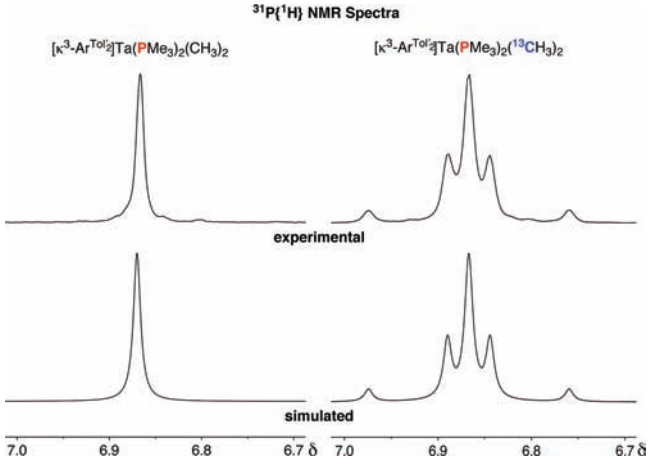

Figure 13. $^{31}P\{^1H\}$ NMR signals for natural abundance $[\kappa^3\text{-}Ar^{Tol'_2}]Ta(PMe_3)_2Me_2$ (left) and ^{13}C-labeled $[\kappa^3\text{-}Ar^{Tol'_2}]Ta(PMe_3)_2(^{13}CH_3)_2$ (right).

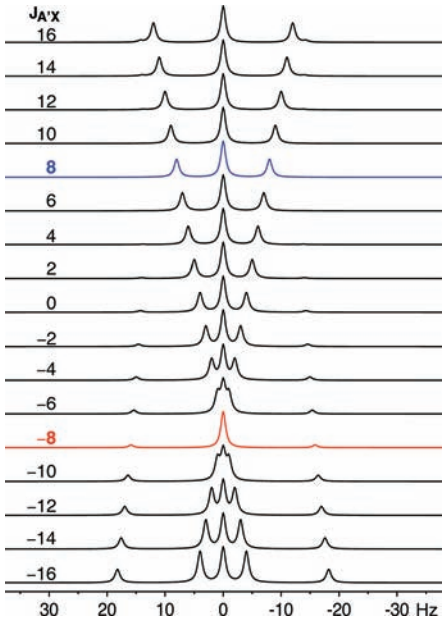

Figure 14. AA′X simulation (X spectrum) as a function of $J_{A'X}$ for fixed $J_{AA'}$ (13.7 Hz) and J_{AX} (8.0 Hz). A non-binomial 1:13.7:1 triplet results when $J_{A'X} = -8.0$ Hz (red), as compared to a binomial 1:2:1 triplet when $J_{A'X} = 8.0$ Hz (blue); A = phosphorus and X = carbon.

as illustrated by the simulation for $^2J_{PP} = |13.7|$ Hz and $^2J_{PC} = \pm 8.0$ Hz (Figure 12, lower left). More complicated patterns are observed if $|J_{AX}| \neq |J_{A'X}|$, and the sensitivity of the X spectrum as a function of varying $J_{A'X}$ is illustrated in Figure 14. On the basis of this simulation, it is evident that one could encounter situations where the signal has the approximate appearance of a binomial triplet (*e.g.*, $J_{AX'} =$ 6 or 10 Hz), but the derived coupling constant would be erroneous.

The tantalum methyl region of the $^{13}C\{^1H\}$ NMR spectrum of isotopically enriched $[\kappa^3\text{-}Ar^{Tol'_2}]Ta(PMe_3)_2(^{13}CH_3)_2$ is a five-line pattern with an intensity ratio 1:4.7:11.4:4.7:1 (Figure 12, right). The latter spectrum is more complicated than that of the natural abundance version (Figure 12, left) because the spin system is now AA′XX′,[34] rather than AA′X. An AA′XX′

dx.doi.org/10.1021/ja210404x | J. Am. Chem.Soc. 2012, 134, 2355−2366

spectrum gives a maximum of 10 lines for each set of nuclei, but this reduces to five lines if $J_{AX} = -J_{AX'}$ and $J_{AA'}$ (or $J_{XX'}$) = 0.[33] Accordingly, the $^{13}C\{^1H\}$ and $^{31}P\{^1H\}$ NMR spectra of $[\kappa^3\text{-}Ar^{Tol'_2}]Ta(PMe_3)_2(^{13}CH_3)_2$ may be simulated satisfactorily with the parameters $^2J_{PP}$ = |13.7| Hz, $^2J_{PC}$ = 8.0 and −8.0 Hz, and $^2J_{CC}$ = 0.0 Hz.[35,36]

As indicated above, the unusual appearance of the tantalum methyl signals in the $^{13}C\{^1H\}$ NMR spectra is a consequence of the two $^2J_{PC}$ coupling constants being of equal magnitude but opposite sign. In this regard, it is well known that $^2J_{XY}$ coupling constants in metal complexes vary with interligand bond angles. For example, the magnitude of $^2J_{PP}$ in metal phosphine compounds is often used to assign a *trans versus cis* stereochemistry by virtue of the fact that *trans* $^2J_{PP}$ coupling constants are generally larger in magnitude than *cis* coupling constants; furthermore, the former are positive and the latter negative.[37] By comparison, there are fewer studies pertaining to $^2J_{CC}$ coupling constants, but it has been observed that *cis* $^2J_{CC}$ coupling constants may be an order of magnitude smaller than *trans* coupling constants and are often not observed.[38] In view of this angular dependence of $^2J_{PP}$ and $^2J_{CC}$ coupling constants, it is not unreasonable that the substantially different P−Ta−C angles [75.1(1)° and 135.1(1)°] for $[\kappa^3\text{-}Ar^{Tol'_2}]Ta(PMe_3)_2Me_2$ would give rise to significantly different $^2J_{PC}$ coupling constants.

Returning to the observation of a singlet in the $^{31}P\{^1H\}$ NMR spectrum of $[\kappa^3\text{-}Ar^{Tol'_2}]Ta(PMe_3)_2Me_2$, but the appearance of an approximate doublet of triplets for the PMe_3 groups in the $^{13}C\{^1H\}$ NMR spectrum (Figure 11), the latter is reconciled by the fact that the presence of a single ^{13}C nucleus causes the phosphorus atoms of the two PMe_3 ligands to become chemically inequivalent due to a secondary isotope effect.[39,40] As such, the $^{13}C\{^1H\}$ NMR signal for the PMe_3 ligands corresponds to an ABX spin system,[41] and the observed spectrum can be simulated by $\Delta\delta_{PP}$ = 0.022 ppm,[42] $^2J_{PP}$ = |13.7| Hz, $^1J_{PC}$ = |21.4| Hz, and $^3J_{PC}$ = 0.0 Hz.[43,44] The impact of $\Delta\delta_{PP}$ on the appearance of the spectrum is illustrated by the simulation shown in Figure 15, in which $^2J_{PP}$ (13.7 Hz), $^1J_{PC}$ (21.4 Hz), and $^3J_{PC}$ (0.0 Hz) are fixed.

It is interesting to note that, in contrast to $[\kappa^3\text{-}Ar^{Tol'_2}]Ta(PMe_3)_2Me_2$, the corresponding $^{13}C\{^1H\}$ NMR spectrum of the dichloride $[\kappa^3\text{-}Ar^{Tol'_2}]Ta(PMe_3)_2Cl_2$ has the appearance of a doublet for the PMe_3 ligands (Figure 16). Despite its appearance, however, the spectrum may be simulated with the parameters $\Delta\delta_{PP}$ = 0.022 ppm,[45] $^2J_{PP}$ = |3.0| Hz, $^1J_{PC}$ = |27.8| Hz, and $^3J_{PC}$ = 0.0 Hz (Figure 16). The fact that it appears as a doublet, rather than a complex six-line pattern similar to that for $[\kappa^3\text{-}Ar^{Tol'_2}]Ta(PMe_3)_2Me_2$, may be attributed to the smaller (but non-zero) value of $^2J_{PP}$, which is presumably a consequence of the fact that the P−Ta−P angle of $[\kappa^3\text{-}Ar^{Tol'_2}]Ta(PMe_3)_2Cl_2$ [139.49(3)°] is smaller than that of $[\kappa^3\text{-}Ar^{Tol'_2}]Ta(PMe_3)_2Me_2$ [144.77(4)°].[37] In this regard, the sensitivity of the appearance of the $^{13}C\{^1H\}$ NMR spectrum to $^2J_{PP}$ is illustrated by the simulation shown in Figure 17, for which $\Delta\delta_{PP}$ (0.022 ppm), $^1J_{PC}$ (21.4 Hz), and $^3J_{PC}$ (0.0 Hz) are fixed with values for $[\kappa^3\text{-}Ar^{Tol'_2}]Ta(PMe_3)_2Me_2$.

Finally, the ^1H NMR spectrum of $[\kappa^3\text{-}Ar^{Tol'_2}]Ta(PMe_3)_2Me_2$ also exhibits some interesting features. For example, while irradiation typically results in spectral simplification, irradiation at the proton frequency of the PMe_3 ligands results in the appearance of *additional* coupling in the ^1H NMR signal for the tantalum methyl groups of $[\kappa^3\text{-}Ar^{Tol'_2}]Ta(PMe_3)_2Me_2$. Specifically, upon irradiation, the doublet takes on the appearance of a "filled-in" doublet (Figure 18). A similar "filled-in" doublet

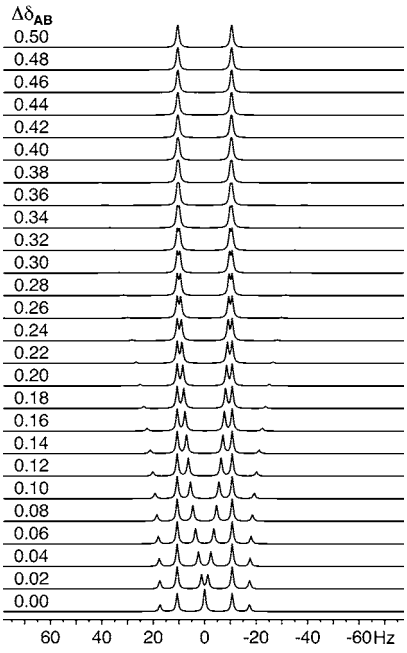

Figure 15. ABX simulation (X spectrum) as a function of $\Delta\delta_{AB}$ for fixed J_{AB} (13.7 Hz), J_{AX} (21.4 Hz), and J_{BX} (0.0 Hz); A = phosphorus, B = phosphorus, and X = carbon.

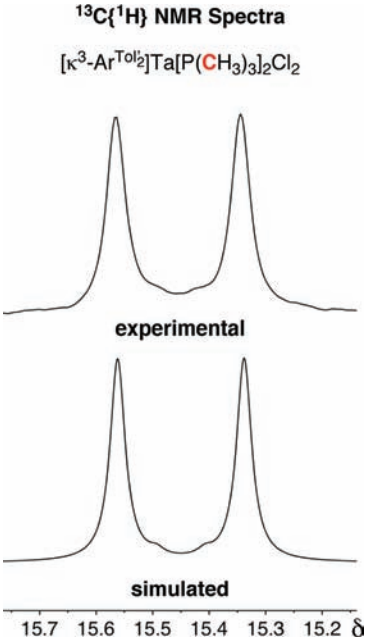

Figure 16. $^{13}C\{^1H\}$ NMR signal for the PMe_3 ligands of $[\kappa^3\text{-}Ar^{Tol'_2}]Ta(PMe_3)_2Cl_2$.

pattern is also observed for the tantalum methyl groups of the $[\kappa^3\text{-}Ar^{Tol'_2}]Ta[P(CD_3)_3]_2Me_2$ isotopologue (Figure 18), and so it is evident that the simpler "doublet" appearance of the non-irradiated spectrum is a result of a small $^5J_{HH}$ coupling between the PMe_3 and TaMe hydrogen atoms, which serves to broaden the features of the "filled-in" doublet.

3. Mechanism for Formation of $[\kappa^3\text{-}Ar^{Tol'_2}]Ta(PMe_3)_2MeCl$. The mechanism for formation of $[\kappa^3\text{-}Ar^{Tol'_2}]Ta(PMe_3)_2MeCl$ is of interest in view of the geometrical constraints that are involved in construction of the pincer ligand.

dx.doi.org/10.1021/ja210404x | J. Am. Chem.Soc. 2012, 134, 2355−2366

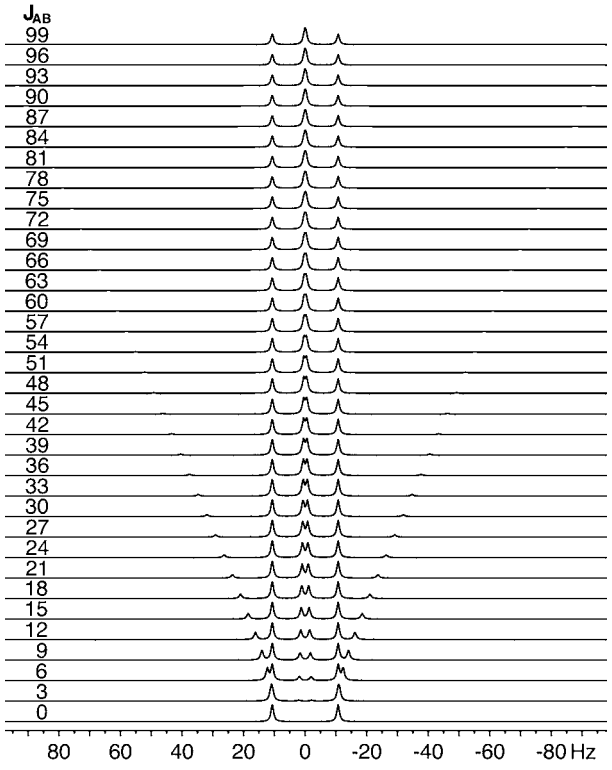

Figure 17. ABX simulation (X spectrum) as a function of J_{AB} for fixed $\Delta\delta_{AB}$ (0.022 ppm), J_{AX} (21.4 Hz), and J_{BX} (0.0 Hz); A = phosphorus, B = phosphorus, and X = carbon.

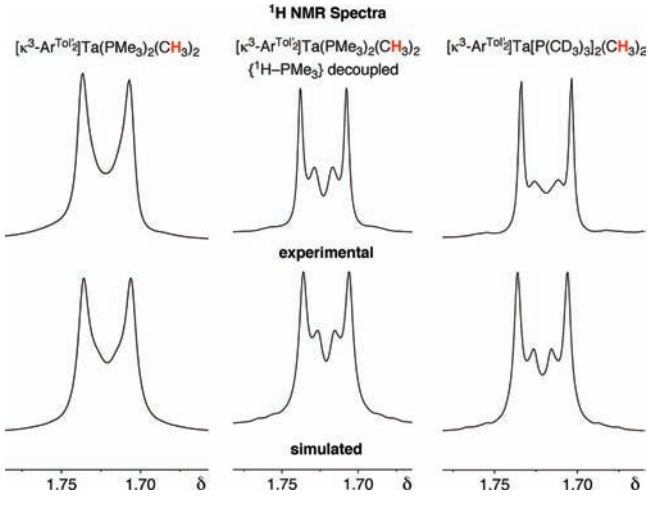

Figure 18. ^{1}H NMR signals for the tantalum methyl groups of [κ^3-Ar$^{Tol'_2}$]Ta(PMe$_3$)$_2$Me$_2$ (left), [κ^3-Ar$^{Tol'_2}$]Ta(PMe$_3$)$_2$Me$_2$ upon selective decoupling of the ^{1}H signals of the PMe$_3$ ligands (center), and the isotopologue [κ^3-Ar$^{Tol'_2}$]Ta[P(CD$_3$)$_3$]$_2$Me$_2$ (right).

In this regard, the simplest mechanistic possibility for creation of the pincer ligand from a [Ar$^{Tol'_2}$]Ta(PMe$_3$)$_x$Me$_3$Cl species involves a pair of Ar–H/Ta–Me sigma-bond metathesis (SBM) transformations, as illustrated in Scheme 4 (in which the PMe$_3$ ligands are omitted for clarity). Another possibility, however, involves elimination of methane by an α-H abstraction process to generate a Ta=CH$_2$ species that subsequently reacts with the C–H bond of an aryl group by a formal 1,2-addition process. For example, (ArO)$_2$TaMe$_3$ (Ar = C$_6$H$_3$Bu$^t_2$) thermally eliminates methane by a sigma-bond metathesis process to give the cyclometalated complex (ArO)(κ^2-OC$_6$H$_3$Bu^t-CMe$_2$CH$_2$)TaMe$_2$, whereas under photochemical conditions (ArO)$_2$TaMe$_3$ eliminates methane *via* α-H abstraction to give the methylidene complex (ArO)$_2$Ta(CH$_2$)Me; the latter complex subsequently converts to (ArO)(κ^2-OC$_6$H$_3$Bu^{t}CMe$_2$CH$_2$)-TaMe$_2$ by 1,2-addition of a methyl C–H bond.[7,46–48] Furthermore, Bercaw has proposed that both sigma-bond metathesis and α-H abstraction processes operate in the elimination of toluene from Ti[(OC$_6$H$_2$-2-Bu^t-4-Me)$_2$C$_6$H$_3$](CH$_2$Ph)$_2$.[5a]

To establish which type of mechanism is responsible for the formation of the pincer ligand, the reaction of the deuterated isotopologue Ta(PMe$_3$)$_2$(CD$_3$)$_3$Cl$_2$ with [Ar^{Tol_2}]Li was investigated. Significantly, the reaction selectively generates CD$_3$H and [κ^3-Ar$^{Tol'_2}$]Ta(PMe$_3$)$_2$(CD$_3$)Cl, both of which are inconsistent with a mechanism that involves α-H abstraction.[49] For example, an α-H abstraction reaction would require both elimination of CD$_4$[50] and a degree of incorporation of ^{1}H into the tantalum methyl group. Conversely, elimination of methane by a sigma-bond metathesis process would liberate only CD$_3$H and result in no incorporation of ^{1}H into the TaMe group. Thus, the observations of (i) CD$_3$H formation (coupled with the absence of CD$_4$) and (ii) no ^{1}H incorporation into the tantalum methyl group provide convincing evidence that the pincer ligand is created by a pair of Ar–H/Ta–Me sigma-bond metathesis transformations.

SUMMARY

In conclusion, a novel [*CCC*] X$_3$-donor pincer ligand has been constructed on tantalum by the PMe$_3$-induced cyclometalation of a terphenyl ligand. The mechanism for the cyclometalation involves a pair of sigma-bond metathesis reactions, and, as such it is possible that this approach may provide a general means for obtaining [*CCC*] X$_3$-donor pincer complexes of other metals and especially those of the early transition elements for which sigma-bond metathesis reactions are common.

EXPERIMENTAL SECTION

General Considerations. All manipulations were performed using a combination of glovebox, high-vacuum, and Schlenk techniques under an argon atmosphere unless otherwise specified.[51] Solvents were purified and degassed by using standard procedures. ^{1}H NMR spectra were measured on Bruker 300 DRX, Bruker 300 DPX, Bruker 400 Avance III, Bruker 400 Cyber-enabled Avance III, and Bruker 500 DMX spectrometers. ^{1}H chemical shifts are reported in ppm relative to SiMe$_4$ (δ = 0) and were referenced internally with respect to the protio solvent impurity (δ 7.16 for C$_6$D$_5$H).[52] ^{13}C NMR spectra are reported in ppm relative to SiMe$_4$ (δ = 0) and were referenced internally with respect to the solvent (δ 128.06 for C$_6$D$_6$).[52] ^{31}P chemical shifts are reported in ppm relative to 85% H$_3$PO$_4$ (δ = 0) and were referenced using P(OMe)$_3$ (δ = 141.0) as an external standard.[53] Coupling constants are given in hertz. NMR spectroscopic simulations were performed using gNMR 5.1 (Adept Scientific) and MestReNova v7.0.3 (Mestrelab Research S.L. 2001), and final images were produced by MestReNova. TaMe$_3$Cl$_2$[9] and Ta(PMe$_3$)$_2$Me$_3$Cl$_2$[22] were prepared by the literature methods. TaCl$_5$, PMe$_3$, ^{13}CH$_3$I, CD$_3$I, and Li wire (0.5–1.0% Na) were obtained commercially from Aldrich. ZnCl$_2$ was obtained from Strem Chemicals and dried with SOCl$_2$ prior to use.[54] Et$_2$O was dried over LiAlH$_4$ and vacuum transferred into an ampoule containing molecular sieves prior to use.

X-ray Structure Determinations. X-ray diffraction data were collected on a Bruker Apex II diffractometer. Crystal data, data collection, and refinement parameters are summarized in the Supporting Information. The structures were solved using direct methods and standard difference map techniques and were refined by full-matrix least-squares procedures on F^2 with SHELXTL (version 6.10).[55]

Computational Details. Calculations were carried out using DFT as implemented in the Jaguar 7.5 (release 207) suite of *ab*

dx.doi.org/10.1021/ja210404x | J. Am. Chem.Soc. 2012, 134, 2355–2366

Scheme 4

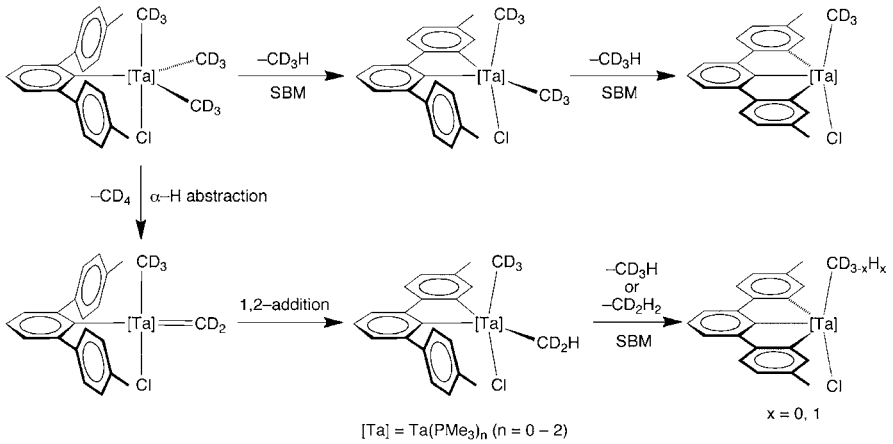

initio quantum chemistry programs.[56] Geometry optimizations were performed with the B3LYP density functional[57] using the 6-31G** (C, H, Cl, and P) and LACVP (Ta) basis sets.[58] The energies of the optimized structures were reevaluated by additional single-point calculations on each optimized geometry using cc-pVTZ(-f) correlation-consistent triple-ζ basis set for C, H, Cl, and P and LACV3P for Ta (see Supporting Information). Molecular orbital analyses were performed with the aid of JIMP2,[28] which employs Fenske–Hall calculations and visualization using MOPLOT.[59]

Synthesis of $Ta(CD_3)_3Cl_2$ and $Ta(PMe_3)_2(CD_3)_3Cl_2$. The synthesis of $Ta(CD_3)_3Cl_2$ was adapted from the literature procedure for $Ta(CH_3)_3Cl_2$.[9c] A solution of CD_3I (2.5 g, 17.2 mmol) in Et_2O (3 mL), cooled to −78 °C to minimize evaporation of CD_3I, was added to a suspension of lithium wire (600 mg, 86 mmol, 0.5–1.0% Na, *ca.* 5 mm pieces) in Et_2O (20 mL) at room temperature over 10 min. The mixture was stirred for 2 h at room temperature and filtered. The filtrate was slowly added to a stirred suspension of $ZnCl_2$ (1.41 g, 10.3 mmol, dried with $SOCl_2$) in Et_2O (5 mL) at −78 °C. After the addition was complete, the suspension was allowed to warm to 0 °C and stirred for 30 min. The *in situ* generated solution of $Zn(CD_3)_2$ in Et_2O was then vapor transferred into a Schlenk tube containing $TaCl_5$ (750 mg, 2.1 mmol) at −196 °C. After the transfer was complete, the mixture was allowed to warm to room temperature and stirred for 2 h. 1,4-Dioxane (0.3 mL, 0.31 g, 3.5 mmol) was added to precipitate $ZnCl_2$·dioxane, which was removed by filtration. The volatile components were removed from the filtrate *in vacuo*, and the resulting pale yellow solid was extracted with pentane (50 mL) and filtered. The pentane was removed from the filtrate *in vacuo* to give $Ta(CD_3)_3Cl_2$ (250 mg, 39% yield). The pale yellow residue of $Ta(CD_3)_3Cl_2$ that could not be removed from the sides of the Schlenk tube was dissolved in pentane (10 mL) and treated with PMe_3 (0.5 mL, 4.9 mmol). The resulting bright yellow suspension was stirred for 20 min, after which the volatile components were removed *in vacuo* to give $Ta(PMe_3)_2(CD_3)_3Cl_2$ (200 mg, 21% yield). The combined yield based on $TaCl_5$ is 60%.

Synthesis of $Ta[P(CD_3)_3]_2Me_3Cl_2$. A solution of $TaMe_3Cl_2$ (350 mg, 1.18 mmol) in pentane (5 mL) was treated with $P(CD_3)_3$ (250 mg, 2.94 mmol, cooled at −15 °C). The resulting bright yellow mixture was shaken for 10 min. After this period, the volatile components were removed *in vacuo* to give $Ta[P(CD_3)_3]_2Me_3Cl_2$ as a bright yellow solid (523 mg, 95% yield).

Synthesis of $[Ar^{Tol_2}]I$. The synthesis of $[Ar^{Tol_2}]I$ was adapted from literature procedures.[60]

(i). Preparation of p-TolMgBr. A degassed solution of *p*-bromotoluene (50.0 g, 0.292 mol) in THF (50 mL) was added slowly over 4 h to a stirred mixture of Mg (10.0 g, 0.411 mol) and THF (250 mL). The mixture was stirred for a further 16 h to generate a solution of the *p*-TolMgBr Grignard reagent.

(ii). Preparation of $[C_6H_3Cl_2]Li$. A solution of 1,3-dichlorobenzene (17.6 g, 0.120 mol) in THF (200 mL) was cooled to −78 °C and treated dropwise with a solution of Bu^nLi in hexanes (52.0 mL, 2.5 M, 0.130 mol) over 3 h, resulting in a yellow-white suspension. The mixture was then stirred for an additional 2 h at −78 °C to generate $[C_6H_3Cl_2]Li$.

(iii). Synthesis of $[Ar^{Tol_2}]I$. The stirred suspension of $[C_6H_3Cl_2]Li$ in THF/hexanes at −78 °C [see section (ii) above] was treated dropwise with the *p*-TolMgBr Grignard reagent [see section (i) above] over 2 h. After the addition, the mixture was allowed to warm slowly to room temperature, stirred for an additional 12 h at room temperature, and then refluxed for 1 h. An aliquot was taken to confirm that the coupling was complete by using ^1H NMR spectroscopy; the aliquot was also used to obtain crystals of $[Ar^{Tol_2}]MgBr(THF)_2$ that were analyzed by X-ray diffraction to confirm the identity of the product (see Supporting Information), although it should be noted that there is disorder with the chloride derivative. The bulk reaction mixture was then cooled to 0 °C, treated slowly with a solution of I_2 (55 g, 0.217 mol) in THF (100 mL) over 20 min, and allowed to warm to room temperature. The mixture was filtered in air through a glass frit to remove the insoluble salts, and the filtrate was washed sequentially with aqueous Na_2SO_3 (2 × 200 mL) and H_2O (2 × 100 mL). The aqueous washings were combined and extracted into Et_2O (200 mL). The ether extract was combined with the original organic layer, which was then dried with $MgSO_4$. The volatile components were removed *in vacuo* to give a light yellow sticky solid that was washed with pentane (3 × 50 mL) and then dried *in vacuo* to give $[Ar^{Tol_2}]I$ as a white powder (28.2 g). The pentane washes were combined and cooled to −15 °C, thereby depositing crystals that were washed with pentane (2 × 10 mL) to give an additional crop of $[Ar^{Tol_2}]I$ (3.7 g). The combined yield of $[Ar^{Tol_2}]I$ is 31.9 g (69%). X-ray-quality crystals of $[Ar^{Tol_2}]I$ were obtained from a solution in pentane at −15 °C (see Supporting Information). Anal. Calcd: C, 62.5; H, 4.5. Found: C, 62.7; H, 4.6. ^1H NMR (C_6D_6): 2.14 [s, 6H of Me of Ar^{Tol_2}], 7.03 [m, 5H of Ar^{Tol_2}], 7.11 [d, $^3J_{H-H}$ = 8, 2H of Ar^{Tol_2}], 7.27 [d, $^3J_{H-H}$ = 8, 4H of Ar^{Tol_2}]. $^{13}C\{^1H\}$ NMR (C_6D_6): 21.2 [s, 2C of Me of Ar^{Tol_2}], 104.8 [s, 1C of Ar^{Tol_2}], 129.0 [s, 3C of Ar^{Tol_2}], 129.7 [s, 4C of Ar^{Tol_2}], 137.2 [s, 2C of Ar^{Tol_2}], 143.5 [s, 2C of Ar^{Tol_2}], 148.9 [s, 2C of Ar^{Tol_2}].

Synthesis of $[Ar^{Tol_2}]Li$. A stirred suspension of $[Ar^{Tol_2}]I$ (5.0 g, 0.013 mol) in pentane (50 mL) was cooled to −78 °C and treated slowly with a solution of Bu^nLi in hexanes (6.77 mL, 2.5 M, 0.017 mol) over 10 min. The mixture was allowed to warm to room temperature over approximately 40 min, after which the volatile components were removed *in vacuo*. The resulting white waxy solid was washed with pentane (2 × 50 mL) and dried *in vacuo* to give $[Ar^{Tol_2}]Li$ as a fine white powder (3.4 g, 99% yield). ^1H NMR (C_6D_6): 2.04 [s, 6H of Me of Ar^{Tol_2}], 6.78 [d, $^3J_{H-H}$ = 8, 4H of Ar^{Tol_2}], 7.34 [d, $^3J_{H-H}$ = 8, 4H of Ar^{Tol_2} and 1H of Ar^{Tol_2} located by COSY], 7.43 [d, $^3J_{H-H}$ = 8, 2H of Ar^{Tol_2}]. $^{13}C\{^1H\}$ NMR (C_6D_6): 20.9 [s, 2C of Me of Ar^{Tol_2}], 124.4 [s, 2C of Ar^{Tol_2}], 126.5 [s, 1C of Ar^{Tol_2}], 126.9 [s, 4C of Ar^{Tol_2}], 131.0 [br s, 4C of Ar^{Tol_2}], 136.4 [s, 2C of Ar^{Tol_2}], 144.7 [s, 2C of Ar^{Tol_2}], 152.1 [s, 2C of Ar^{Tol_2}], 175.4 [s, 1C of Ar^{Tol_2}, not observed, located using 2D HMBC].

dx.doi.org/10.1021/ja210404x | *J. Am. Chem.Soc.* 2012, 134, 2355–2366

Synthesis of [Ar^{Tol_2}]TaMe$_3$Cl. A pale yellow solution of $TaMe_3Cl_2$ (60 mg, 0.20 mmol) in Et_2O (1 mL) at −15 °C was treated with a suspension of [Ar^{Tol_2}]Li (60 mg, 0.23 mmol) in Et_2O (2 mL) at −15 °C, resulting in the immediate formation of a dark brown suspension. The volatile components were removed *in vacuo*, resulting in a brown solid that was washed with pentane (3 × 1 mL) and then extracted into benzene (2 × 0.5 mL). The solution was lyophilized to give [Ar^{Tol_2}]TaMe$_3$Cl as an orange-brown powder (22 mg, 21% yield). X-ray-quality crystals were obtained from slow evaporation of a solution in pentane at room temperature. Anal. Calcd: C, 53.24; H, 5.05. Found: C, 54.06; H, 5.04. ^{1}H NMR (C_6D_6): 0.86 [s, 9H of Ta*Me*$_3$], 2.09 [s, 6H of Me of Ar^{Tol_2}], 7.06 [d, $^3J_{H-H}$ = 7, 4H of Ar^{Tol_2}], 7.22 [t, $^3J_{H-H}$ = 8, 1H of Ar^{Tol_2}], 7.31 [d, $^3J_{H-H}$ = 8, 2H of Ar^{Tol_2}], 7.72 [d, $^3J_{H-H}$ = 7, 4H of Ar^{Tol_2}]. ^{13}C{^{1}H} NMR (C_6D_6): 21.2 [s, 2C of Me of Ar^{Tol_2}], 86.4 [very br, 3C of Ta*Me*$_3$, supported by HSQC spectroscopy], 129.1 [s, 2C of Me of Ar^{Tol_2}], 130.4 [s, 4C of Me of Ar^{Tol_2}], 131.4 [s, 1C of Me of Ar^{Tol_2}], 131.4 [s, 4C of Me of Ar^{Tol_2}], 138.1 [s, 2C of Me of Ar^{Tol_2}], 139.2 [s, 2C of Me of Ar^{Tol_2}], 145.1 [s, 2C of Me of Ar^{Tol_2}], 216.1 [s, 1C of Me of Ar^{Tol_2}].

Decomposition of [Ar^{Tol_2}]TaMe$_3$Cl to [Ar^{Tol_2}]TaMe$_2$Cl$_2$. A solution of [Ar^{Tol_2}]TaMe$_3$Cl in d_6-benzene decomposes at room temperature to produce, *inter alia*, [Ar^{Tol_2}]TaMe$_2$Cl$_2$ and methane over several days. X-ray-quality crystals were obtained from a solution in pentane at −15 °C. ^{1}H NMR (C_6D_6): 1.06 [s, 6H of Ta*Me*$_2$], 2.06 [s, 6H of Me of Ar^{Tol_2}], 6.98 [d, $^3J_{H-H}$ = 8, 4H of Ar^{Tol_2}], 7.16 [1H of Ar^{Tol_2}, under C_6D_5H signal], 7.22 [d, $^3J_{H-H}$ = 7, 2H of Ar^{Tol_2}], 7.67 [d, $^3J_{H-H}$ = 8, 4H of Ar^{Tol_2}],

Synthesis of [κ^3-Ar$^{Tol_2'}$]Ta(PMe$_3$)$_2$MeCl. A solution of Ta(PMe$_3$)$_2$Me$_3$Cl$_2$ (50 mg, 0.11 mmol) in d_6-benzene (*ca.* 1 mL) in a vial was treated with [Ar^{Tol_2}]Li (50 mg, 0.19 mmol). After 5 min, the mixture was filtered through Celite into an NMR tube equipped with a J. Young valve and then allowed to sit at room temperature for 12 h. After this period, the mixture was lyophilized, washed with pentane (3 × 1 mL), extracted into d_6-benzene (2 × 0.5 mL), and filtered through Celite. The filtrate was analyzed by ^{1}H and ^{31}P{^{1}H} NMR spectroscopy, thereby demonstrating the formation of [κ^3-Ar$^{Tol_2'}$]Ta(PMe$_3$)$_2$MeCl. The solution was lyophilized to give [κ^3-Ar$^{Tol_2'}$]Ta(PMe$_3$)$_2$MeCl as an orange-brown powder (34 mg, 48% yield). X-ray-quality crystals were obtained from a solution in pentane at −15 °C. It should be noted, however, that the methyl and chloride ligands are disordered. Furthermore, in solution, [κ^3-Ar$^{Tol_2'}$]Ta(PMe$_3$)$_2$MeCl is in equilibrium with [κ^3-Ar$^{Tol_2'}$]Ta(PMe$_3$)$_2$Cl$_2$ and [κ^3-Ar$^{Tol_2'}$]Ta(PMe$_3$)$_2$Me$_2$ ($K \approx 5 \times 10^{-2}$). The disorder was modeled such that the Ta−Me and the Ta−Cl ligands each have a total occupancy of 1. Anal. Calcd: C, 50.76; H, 5.68. Found: C, 50.03; H, 5.41. ^{1}H NMR (C_6D_6): 0.42 [d, $^2J_{P-H}$ = 9, 9H of (P*Me*$_3$)$_2$], 0.53 [d, $^2J_{P-H}$ = 9, 9H of (P*Me*$_3$)$_2$], 2.00 [d, $^3J_{P-H}$ = 12, 3H of Ta*Me*], 2.23 [s, 6H of Me of Ar$^{Tol_2'}$], 7.08 [d, $^3J_{H-H}$ = 7, 2H of Ar$^{Tol_2'}$], 7.36 [t, $^3J_{H-H}$ = 8, 1H of Ar$^{Tol_2'}$], 7.62 [d, $^3J_{H-H}$ = 8, 2H of Ar$^{Tol_2'}$], 7.75 [d, $^3J_{H-H}$ = 7, 2H of Ar$^{Tol_2'}$], 7.82 [s, 2H of Ar$^{Tol_2'}$]. ^{31}P{^{1}H} NMR (C_6D_6): 9.0 [d, $^2J_{P-P}$ = 10, 1P of (P*Me*$_3$)$_2$], 17.3 [d, $^2J_{P-P}$ = 10, 1P of (P*Me*$_3$)$_2$]. ^{13}C{^{1}H} NMR (C_6D_6): 14.5 [d, $^1J_{P-C}$ = 24, 3C of (P*Me*$_3$)$_2$], 15.0 [d, $^1J_{P-C}$ = 25, 3C of (P*Me*$_3$)$_2$], 21.8 [s, 2C of Me of Ar$^{Tol_2'}$], 75.9 [dd, $^2J_{P-C}$ = 13, $^2J_{P-C}$ = 9, 1C of Ta*Me*], 119.4 [t, J_{P-C} = 3, 2C of Ar$^{Tol_2'}$], 121.3 [s, 2C of Ar$^{Tol_2'}$], 128.0 [s, 1C of Ar$^{Tol_2'}$, under C_6D_6, located by HSQC spectroscopy], 129.1 [s, 2C of Ar$^{Tol_2'}$], 133.5 [s, 2C of Ar$^{Tol_2'}$], 139.9 [s, 2C of Ar$^{Tol_2'}$], 152.8 [s, 2C of Ar$^{Tol_2'}$], 156.4 [t, $^2J_{P-C}$ = 3, 2C of Ar$^{Tol_2'}$], 198.8 [dd, $^2J_{P-C}$ = 26, $^2J_{P-C}$ = 19, 1C of Ar$^{Tol_2'}$], 204.8 [dd, $^2J_{P-C}$ = 11, $^2J_{P-C}$ = 8, 2C of Ar$^{Tol_2'}$].

Reaction between Ta(PMe$_3$)$_2$(CD$_3$)$_3$Cl$_2$ and [Ar^{Tol_2}]Li. *A.* A solution of Ta(PMe$_3$)$_2$(CD$_3$)$_3$Cl$_2$ (20 mg, 0.04 mmol) in d_6-benzene (*ca.* 0.7 mL) in a vial was treated with [Ar^{Tol_2}]Li (18 mg, 0.07 mmol) and filtered quickly through Celite into an NMR tube equipped with a J. Young valve that was closed following the transfer. The solution was analyzed by ^{1}H NMR spectroscopy, thereby demonstrating the rapid formation of CD_3H. In addition, there were no signals attributable to the methyl groups of [κ^3-Ar$^{Tol_2'}$]Ta(PMe$_3$)$_2$Me$_2$ and [κ^3-Ar$^{Tol_2'}$]Ta(PMe$_3$)$_2$MeCl, consistent with the presence of [κ^3-Ar$^{Tol_2'}$]Ta(PMe$_3$)$_2$(CD$_3$)$_2$ and [κ^3-Ar$^{Tol_2'}$]Ta(PMe$_3$)$_2$(CD$_3$)Cl isotopologues.

B. A solution of Ta(PMe$_3$)$_2$(CD$_3$)$_3$Cl$_2$ (20 mg, 0.04 mmol) in benzene (*ca.* 0.7 mL) in a vial was treated with [Ar^{Tol_2}]Li (18 mg, 0.07 mmol). The vial was capped with a suba seal, shaken for 1 min, and then allowed to stand at room temperature for 30 min. The gas above the solution was then collected using a 1 mL gastight microsyringe and injected into the mass spectrometer (electron ionization (EI) method, 70 eV ionization energy through gas inlet reservoir; HX110 double-focusing mass spectrometer, JEOL Ltd., Tokyo, Japan). The spectra displayed a signal at m/z = 19 (CD_3H) and no signal at m/z = 20 (CD_4), thereby providing further evidence for the presence of CD_3H, with no evidence for CD_4. After the first analysis, another 1 mL of gas was collected and the experiment repeated, giving consistent results.

Reaction between Ta[P(CD$_3$)$_3$]$_2$Me$_3$Cl$_2$ and [Ar^{Tol_2}]Li. A solution of Ta[P(CD$_3$)$_3$]$_2$Me$_3$Cl$_2$ (20 mg, 0.04 mmol) in d_6-benzene (*ca.* 0.7 mL) was treated with [Ar^{Tol_2}]Li (18 mg, 0.07 mmol). The mixture was shaken for 1 min, filtered through Celite into an NMR tube equipped with a J. Young valve, and allowed to stand at room temperature for 12 h. The solution was analyzed by ^{1}H NMR spectroscopy, thereby demonstrating the formation of [κ^3-Ar$^{Tol_2'}$]Ta[P(CD$_3$)$_3$]$_2$MeCl. This solution was treated with PMe_3 (0.05 mL) and monitored by ^{1}H NMR spectroscopy, thereby demonstrating PMe_3/P(CD$_3$)$_3$ exchange over 12 h.

Conversion of [Ar^{Tol_2}]TaMe$_3$Cl to [κ^3-Ar$^{Tol_2'}$]Ta(PMe$_3$)$_2$MeCl. A solution of [Ar^{Tol_2}]TaMe$_3$Cl (22 mg, 0.04 mmol) in d_6-benzene in an NMR tube equipped with a J. Young valve was treated with PMe_3 (*ca.* 0.05 mL) *via* vapor transfer. The reaction was monitored by ^{1}H and ^{31}P{^{1}H} NMR spectroscopy, thereby demonstrating the formation of [κ^3-Ar$^{Tol_2'}$]Ta(PMe$_3$)$_2$MeCl as the major product, in addition to a small quantity of Ar^{Tol_2}H (<10%). The sample was lyophilized, washed with pentane (2 × 1 mL), and extracted into benzene (2 × 0.5 mL). The solution was lyophilized to give [κ^3-Ar$^{Tol_2'}$]Ta(PMe$_3$)$_2$MeCl as an orange powder (17 mg, 63% yield).

Reaction between [Ar^{Tol_2}]Ta(CD$_3$)$_3$Cl and PMe$_3$. A solution of Ta(CD$_3$)$_3$Cl$_2$ (20 mg, 0.07 mmol) in d_6-benzene (*ca.* 0.7 mL) was treated with [Ar^{Tol_2}]Li (18 mg, 0.07 mmol). The mixture was shaken for 1 min and then filtered through Celite into an NMR tube equipped with a J. Young valve. The sample was analyzed by ^{1}H NMR spectroscopy, demonstrating the immediate conversion to, *inter alia*, [Ar^{Tol_2}]Ta(CD$_3$)$_3$Cl. PMe_3 (0.05 mL) was added *via* vapor transfer and the solution analyzed by ^{1}H NMR spectroscopy, thereby demonstrating the immediate formation of CD_3H. In addition, there were no signals attributable to the methyl groups of [κ^3-Ar$^{Tol_2'}$]Ta(PMe$_3$)$_2$Me$_2$ and [κ^3-Ar$^{Tol_2'}$]Ta(PMe$_3$)$_2$MeCl, consistent with the presence of [κ^3-Ar$^{Tol_2'}$]Ta(PMe$_3$)$_2$(CD$_3$)$_2$ and [κ^3-Ar$^{Tol_2'}$]Ta(PMe$_3$)$_2$(CD$_3$)Cl isotopologues.

Synthesis of [κ^3-Ar$^{Tol_2'}$]Ta(PMe$_3$)$_2$Cl$_2$. A solution of [κ^3-Ar$^{Tol_2'}$]Ta(PMe$_3$)$_2$MeCl (25 mg, 0.04 mmol) in d_6-benzene (*ca.* 0.7 mL) in an NMR tube equipped with a J. Young valve was treated with a suspension of $ZnCl_2$ (25 mg, 0.18 mmol) in Et_2O (*ca.* 0.1 mL). The sample was lyophilized after 1 h, extracted into benzene, and filtered into an NMR tube. The sample was treated with PMe_3 (*ca.* 0.05 mL) and analyzed by ^{1}H NMR spectroscopy, thereby demonstrating the formation of [κ^3-Ar$^{Tol_2'}$]Ta(PMe$_3$)$_2$Cl$_2$. The sample was then lyophilized, and the residue obtained was washed with pentane (1 mL), extracted into benzene (2 × 0.7 mL), and lyophilized to give [κ^3-Ar$^{Tol_2'}$]Ta(PMe$_3$)$_2$Cl$_2$ as a red powder (11 mg, 42% yield). X-ray-quality crystals of [κ^3-Ar$^{Tol_2'}$]Ta(PMe$_3$)$_2$Cl$_2$ were obtained from a solution in pentane at −15 °C. Anal. Calcd: C, 47.4; H, 5.0. Found: C, 47.6; H, 4.8. ^{1}H NMR (C_6D_6): 0.54 [d, $^2J_{P-H}$ = 10, 18H of (P*Me*$_3$)$_2$], 2.16 [s, 6H of Me of Ar$^{Tol_2'}$], 7.08 [d, $^3J_{H-H}$ = 8, 2H of Ar$^{Tol_2'}$], 7.32 [t, $^3J_{H-H}$ = 8, 1H of Ar$^{Tol_2'}$], 7.61 [d, $^3J_{H-H}$ = 8, 2H of Ar$^{Tol_2'}$], 7.70 [d, $^3J_{H-H}$ = 7, 2H of Ar$^{Tol_2'}$], 8.27 [s, 2H of Ar$^{Tol_2'}$]. ^{31}P{^{1}H} NMR (C_6D_6): 20.2 [s, 2P of (P*Me*$_3$)$_2$]. ^{13}C{^{1}H} NMR (C_6D_6): 15.5 [apparent doublet, $^1J_{P-C}$ = 27.75, $^2J_{P-P}$ = 3.0, $^3J_{P-C}$ = 0, δ_{P-P} = 0.022 (see Figure 16 for simulation), 6C of (P*Me*$_3$)$_2$], 21.7 [s, 2C of Me of Ar$^{Tol_2'}$], 120.3 [s, 2C of Ar$^{Tol_2'}$], 121.2 [s, 2C of Ar$^{Tol_2'}$], 128.0 [s, 1C of Ar$^{Tol_2'}$, under C_6D_6, located by HSQC spectroscopy], 130.4 [s, 2C of Ar$^{Tol_2'}$], 133.9 [s, 2C of Ar$^{Tol_2'}$], 141.6 [s, 2C of Ar$^{Tol_2'}$], 152.0

dx.doi.org/10.1021/ja210404x | *J. Am. Chem.Soc.* 2012, 134, 2355−2366

[s, 2C of $Ar^{Tol'_2}$], 156.6 [s, 2C of $Ar^{Tol'_2}$], 201.5 [t, $^2J_{P-C}$ = 25, 1C of $Ar^{Tol'_2}$], 206.4 [t, $^2J_{P-C}$ = 9, 2C of $Ar^{Tol'_2}$].

Synthesis of [κ^3-$Ar^{Tol'_2}$]Ta(PMe_3)$_2$$Me_2$. *A.* A solution of Ta($PMe_3$)$_2$$Me_3Cl_2$ (50 mg, 0.11 mmol) in d_6-benzene (*ca.* 1 mL) in a vial was treated with [Ar^{Tol_2}]Li (50 mg, 0.19 mmol). After 5 min, the mixture was filtered through Celite into an NMR tube equipped with a J. Young valve and then allowed to sit at room temperature for 12 h to generate [κ^3-$Ar^{Tol'_2}$]Ta(PMe_3)$_2$MeCl. After this period, MeMgBr (20 mg, 0.17 mmol) was added, and the tube was shaken and allowed to sit at room temperature for 4 h. The mixture was then lyophilized, and the residue obtained was washed with pentane (3 × 1 mL) and extracted into benzene (2 × 0.5 mL). The solution was lyophilized to give [κ^3-$Ar^{Tol'_2}$]Ta(PMe_3)$_2$$Me_2$ as an orange-brown powder (32 mg, 46% yield). X-ray-quality crystals of [κ^3-$Ar^{Tol'_2}$]Ta(PMe_3)$_2$$Me_2$ were obtained from a solution in pentane at −15 °C. ^{1}H NMR (C_6D_6): 0.46 [m, 18H of (PMe_3)$_2$], 1.73 [m, 6H of TaMe_2], 2.29 [s, 6H of Me of $Ar^{Tol'_2}$], 7.10 [d, $^3J_{H-H}$ = 8, 2H of $Ar^{Tol'_2}$], 7.37 [t, $^3J_{H-H}$ = 8, 1H of $Ar^{Tol'_2}$], 7.61 [d, $^3J_{H-H}$ = 8, 2H of $Ar^{Tol'_2}$], 7.67 [s, 2H of $Ar^{Tol'_2}$], 7.77 [d, $^3J_{H-H}$ = 8, 2H of $Ar^{Tol'_2}$]. ^{31}P{^{1}H} NMR (C_6D_6): 6.9 [s, 2P of (PMe_3)$_2$]. ^{13}C{^{1}H} NMR (C_6D_6): 14.3 [m, 6C of (PMe_3)$_2$], 21.9 [s, 2C of Me of $Ar^{Tol'_2}$], 77.7 [m, 2C of TaMe_2], 118.7 [t, J_{P-C} = 3, 2C of $Ar^{Tol'_2}$], 121.3 [s, 2C of $Ar^{Tol'_2}$], 127.6 [t, J_{P-C} = 3, 2C of $Ar^{Tol'_2}$], 128.0 [s, 1C of $Ar^{Tol'_2}$, under C_6D_6, located by HSQC spectroscopy], 133.2 [s, 2C of $Ar^{Tol'_2}$], 138.1 [s, 2C of $Ar^{Tol'_2}$], 153.6 [s, 2C of $Ar^{Tol'_2}$], 156.9 [t, J_{P-C} = 3, 2C of $Ar^{Tol'_2}$], 198.2 [t, $^2J_{P-C}$ = 21, 1C of $Ar^{Tol'_2}$], 206.9 [t, $^2J_{P-C}$ = 8, 2C of $Ar^{Tol'_2}$].

B. A mixture of [κ^3-$Ar^{Tol'_2}$]Ta(PMe_3)$_2$$Cl_2$ (10 mg, 0.02 mmol) and MeMgBr (4 mg, 0.03 mmol) in an NMR tube equipped with a J. Young valve was treated with d_6-benzene (*ca.* 0.7 mL) and Et_2O (*ca.* 0.05 mL). The reaction was monitored by ^{1}H NMR spectroscopy, thereby demonstrating conversion to [κ^3-$Ar^{Tol'_2}$]Ta(PMe_3)$_2$$Me_2$ over a period of less than 10 min.

Synthesis of ($^{13}CH_3$)MgI·(Et_2O)$_{1.5}$. A stirred suspension of Mg turnings (0.85 g, 35.0 mmol) in Et_2O (7 mL) was treated with $^{13}CH_3I$ (1.0 g, 7.0 mmol) and stirred for 2 h at room temperature. After this period, the mixture was filtered, and the volatile components were removed from the filtrate *in vacuo* to give ($^{13}CH_3$)MgI·(Et_2O)$_{1.5}$ as a white powder (1.20 g, 62% yield). ^{1}H NMR (C_6D_6): −0.41 [d, $^1J_{C-H}$ = 105, 3H of $^{13}CH_3$MgI], 0.78 [t, $^3J_{H-H}$ = 7, 9H of (Et_2O)$_{1.5}$], 3.36 [q, $^3J_{H-H}$ = 7, 6H of (Et_2O)$_{1.5}$]. ^{13}C{^{1}H} NMR (C_6D_6): −9.2 [s, 1C of $^{13}CH_3$MgI], 14.1 [s, 3C of (Et_2O)$_{1.5}$], 66.7 [s, 3C of (Et_2O)$_{1.5}$].

Synthesis of [κ^3-$Ar^{Tol'_2}$]Ta(PMe_3)$_2$($^{13}CH_3$)$_2$. A mixture of [κ^3-$Ar^{Tol'_2}$]Ta(PMe_3)$_2$$Cl_2$ (10 mg, 0.02 mmol) and ($^{13}CH_3$)MgI·(Et_2O)$_{1.5}$ (5 mg, 0.02 mmol) in an NMR tube equipped with a J. Young valve was treated with d_6-benzene (*ca.* 0.7 mL). The reaction was monitored by ^{1}H NMR spectroscopy, thereby demonstrating conversion to [κ^3-$Ar^{Tol'_2}$]Ta(PMe_3)$_2$($^{13}CH_3$)$_2$ over a period of less than 10 min. The mixture was lyophilized, and the residue was extracted into d_6-benzene for analysis by multinuclear NMR spectroscopy. Selected ^{1}H NMR (C_6D_6): 1.72 [dm, $^1J_{C-H}$ = 117, 6H of Ta($^{13}CH_3$)$_2$].

Synthesis of [κ^3-$Ar^{Tol'_2}$]Ta(PMe_3)$_2$($^{13}CH_3$)$_{2-x}$(Me)$_x$. A mixture of [κ^3-$Ar^{Tol'_2}$]Ta(PMe_3)$_2$MeCl (10 mg, 0.02 mmol) and ($^{13}CH_3$)MgI·(Et_2O)$_{1.5}$ (3 mg, 0.01 mmol) in an NMR tube equipped with a J. Young valve was treated with d_6-benzene (*ca.* 0.7 mL). The reaction was monitored by ^{1}H NMR spectroscopy, thereby demonstrating conversion to a mixture of isotopologues, [κ^3-$Ar^{Tol'_2}$]Ta(PMe_3)$_2$($^{13}CH_3$)$_{2-x}$(Me)$_x$ (x = 0, 1, 2), over a period of less than 10 min. The mixture was lyophilized, and the residue obtained was extracted into d_6-benzene for analysis by multinuclear NMR spectroscopy. Simulation of the ^{13}C{^{1}H} and ^{31}P{^{1}H} NMR spectra (see Supporting Information) identified that the mixture of isopologues consisted of [κ^3-$Ar^{Tol'_2}$]Ta(PMe_3)$_2$($^{13}CH_3$)$_2$ (25%), [κ^3-$Ar^{Tol'_2}$]Ta(PMe_3)$_2$($^{13}CH_3$)($^{12}CH_3$) (50%), and [κ^3-$Ar^{Tol'_2}$]Ta(PMe_3)$_2$($^{12}CH_3$)$_2$ (25%). Selected ^{1}H NMR (C_6D_6) for the mixture of three isotopologues: 1.72 [dm, $^1J_{C-H}$ = 117, 6H of Ta($^{13}CH_3$)$_2$]; 1.72 [dm, $^1J_{C-H}$ = 117, 3H of Ta($^{13}CH_3$)Me], 1.72 [m, 3H of Ta($^{13}CH_3$)*Me*]; 1.72 [m, 6H of TaMe_2].

Synthesis of [κ^3-$Ar^{Tol'_2}$]Ta(PMe_3)$_2$(η^6-C_6H_6). A solution of [κ^3-$Ar^{Tol'_2}$]Ta(PMe_3)$_2$$Cl_2$ (30 mg, 0.05 mmol) in benzene (*ca.* 1 mL) in a vial equipped with a stir bar was treated with KC_8 (30 mg, 0.22 mmol). The resulting mixture was stirred for 1 h, filtered and the filtrate was lyophilized. The sample was extracted into pentane (1 mL) and cooled at −15 °C, thereby depositing red crystals of [κ^3-$Ar^{Tol'_2}$]Ta(PMe_3)$_2$(η^6-C_6H_6) (*ca.* 3 mg), in addition to colorless crystals of [Ar^{Tol_2}]H. X-ray-quality crystals of [κ^3-$Ar^{Tol'_2}$]Ta(PMe_3)$_2$(η^6-C_6H_6) were obtained from a solution in hexane at −15 °C. ^{1}H NMR (C_6D_6): 0.27 [vt, $^2J_{P-H}$ = 8, 18H of (PMe_3)$_2$], 2.44 [s, 6H of Me of $Ar^{Tol'_2}$], 4.10 [t, J_{P-H} = 2, 6H of (η^6-C_6H_6)], 7.11 [d, $^3J_{H-H}$ = 8, 2H of $Ar^{Tol'_2}$], 7.43 [m, 3H of $Ar^{Tol'_2}$], 7.81 [d, $^3J_{H-H}$ = 8, 2H of $Ar^{Tol'_2}$], 7.93 [d, $^3J_{H-H}$ = 8, 2H of $Ar^{Tol'_2}$]. ^{31}P{^{1}H} NMR (C_6D_6): −29.3 [s, 2P of (PMe_3)$_2$]. Selected ^{13}C{^{1}H} NMR located by 2D HSQC experiment (C_6D_6): 98.7 [6C of (η^6-C_6H_6)], 16.2 [6C of (PMe_3)$_2$].

■ ASSOCIATED CONTENT

Ⓢ Supporting Information

Tables of crystallographic data, CIF files, and Cartesian coordinates for geometry-optimized structures and additional NMR data for [κ^3-$Ar^{Tol'_2}$]Ta(PMe_3)$_2$$Me_2$ isotopologues. This material is available free of charge *via* the Internet at http://pubs.acs.org.

■ AUTHOR INFORMATION

Corresponding Author

parkin@columbia.edu

■ ACKNOWLEDGMENTS

We thank the U.S. Department of Energy, Office of Basic Energy Sciences (DE-FG02-93ER14339), for support of this research. The National Science Foundation (CHE-0840451) is thanked for acquisition of an NMR spectrometer. Yi Rong is thanked for helpful discussion.

■ REFERENCES

(1) (a) Choi, J.; MacArthur, A. H. R.; Brookhart, M.; Goldman, A. S. *Chem. Rev.* **2011**, *111*, 1761−1779. (b) Albrecht, M.; Lindner, M. M. *Dalton Trans.* **2011**, *40*, 8733−8744. (c) Leis, W.; Mayer, H. A.; Kaska, W. C. *Coord. Chem. Rev.* **2008**, *252*, 1787−1797. (d) van der Boom, M. E.; Milstein, D. *Chem. Rev.* **2003**, *103*, 1759−1792. (e) Albrecht, M.; van Koten, G. *Angew. Chem., Int. Ed.* **2001**, *40*, 3750−3781. (f) Pugh, D.; Danopoulos, A. A. *Coord. Chem. Rev.* **2007**, *251*, 610−641. (g) Benito-Garagorri, D.; Kirchner, K. *Acc. Chem. Res.* **2008**, *41*, 201−213. (h) Nishiyama, H. *Chem. Soc. Rev.* **2007**, *36*, 1133−1141. (i) van der Vlugt, J. I.; Reek, J. N. H. *Angew. Chem., Int. Ed.* **2009**, *48*, 8832−8846. (j) Liang, L.-C. *Coord. Chem. Rev.* **2006**, *250*, 1152−1177. (k) van Koten, G. *Pure Appl. Chem.* **1989**, *61*, 1681−1694. (l) Fryzuk, M. D.; Montgomery, C. D. *Coord. Chem. Rev.* **1989**, *95*, 1−40. (m) Fryzuk, M. D. *Can. J. Chem.* **1992**, *70*, 2839−2845. (n) Moughton, A. O.; O'Reilly, R. K. *Macromol. Rapid Commun.* **2010**, *31*, 37−52. (o) Wieczorek, B.; Dijkstra, H. P.; Egmond, M. R.; Klein Gebbink, R. J. M.; van Koten, G. *J. Organomet. Chem.* **2009**, *694*, 812−822. (p) *The Chemistry of Pincer Compounds*; Morales-Morales, D., Jensen, C. M., Eds.; Elsevier: Amsterdam, 2007.

(2) (a) Green, M. L. H. *J. Organomet. Chem.* **1995**, *500*, 127−148. (b) Parkin, G. In *Comprehensive Organometallic Chemistry III*; Crabtree, R. H., Mingos, D. M. P., Eds.; Elsevier: Oxford, 2006; Vol. *1*, Chapter 1.01.

(3) For examples of L_2X [*CCC*] pincer ligands, see: (a) Chianese, A. R.; Mo, A.; Lampland, N. L.; Swartz, R. L.; Bremer, P. T. *Organometallics* **2010**, *29*, 3019−3026. (b) Lv, K.; Cui, D. *Organometallics* **2008**, *27*, 5438−5440. (c) Lv, K.; Cui, D. *Organometallics* **2010**, *29*, 2987−2993. (d) Liu, A.; Zhang, X.; Chen, W. *Organometallics* **2009**, *28*, 4868−4871. (e) Gründemann, S.; Albrecht, M.; Loch, J. A.; Faller, J. W.; Crabtree, R. H. *Organometallics* **2001**, *20*, 5485−5488. (f) Cho, J.; Hollis, T. K.; Valente, E. J.; Trate, J. M. *J. Organomet. Chem.* **2011**, *696*, 373−377. (g) Cho, J.; Hollis, T. K.; Helgert, T. R.; Valente, E. J. *Chem. Commun.* **2008**, 5001−5003. (h) Bauer, E. B.; Andavan, G. T. S.; Hollis, T. K.; Rubio, R. J.; Cho, J.; Kuchenbeiser, G. R.; Helgert, T. R.; Letko, C. S.; Tham, F. S. *Org. Lett.*

2008, *10*, 1175−1178. (i) Andavan, G. T. S.; Bauer, E. B.; Letko, C. S.; Hollis, T. K.; Tham, F. S. *J. Organomet. Chem.* **2005**, *690*, 5938−5947. (j) Rubio, R. J.; Andavan, G. T. S.; Bauer, E. B.; Hollis, T. K.; Cho, J.; Tham, F. S.; Donnadieu, B. *J. Organomet. Chem.* **2005**, *690*, 5353−5364.

(4) For examples of LX_2 [*CCC*] pincer and related ligands, see: (a) Stylianides, N.; Danopoulos, A. A.; Pugh, D.; Hancock, F.; Zanotti-Gerosa, A. *Organometallics* **2007**, *26*, 5627−5635. (b) Navarro, J.; Torres, O.; Martín, M.; Sola, E. *J. Am. Chem. Soc.* **2011**, *133*, 9738−9740.

(5) For some recent illustrations of X_3 pincer ligands that feature other donor arrays, *e.g.*, [*OCO*], [*NCN*], and [*ONO*], see: (a) Golisz, S. R.; Labinger, J. A.; Bercaw, J. E. *Organometallics* **2010**, *29*, 5026−5032. (b) Kuppuswamy, S.; Ghiviriga, I.; Abboud, K. A.; Veige, A. S. *Organometallics* **2010**, *29*, 6711−6722. (c) Kuppuswamy, S.; Peloquin, A. J.; Ghiviriga, I.; Abboud, K. A.; Veige, A. S. *Organometallics* **2010**, *29*, 4227−4233. (d) Sarkar, S.; McGowan, K. P.; Culver, J. A.; Carlson, A. R.; Koller, J.; Peloquin, A. J.; Veige, M. K.; Abboud, K. A.; Veige, A. S. *Inorg. Chem.* **2010**, *49*, 5143−5156. (e) Nguyen, A. I.; Blackmore, K. J.; Carter, S. M.; Zarkesh, R. A.; Heyduk, A. F. *J. Am. Chem. Soc.* **2009**, *131*, 3307−3316. (f) Nguyen, A. I.; Zarkesh, R. A.; Lacy, D. C.; Thorson, M. K.; Heyduk, A. F. *Chem. Sci.* **2011**, *2*, 166−169. (g) Zarkesh, R. A.; Heyduk, A. F. *Organometallics* **2009**, *28*, 6629−6631. (h) Korobkov, I.; Gorelsky, S.; Gambarotta, S. *J. Am. Chem. Soc.* **2009**, *131*, 10406−10420. (i) O'Reilly, M.; Falkowski, J. M.; Ramachandran, V.; Pati, M.; Abboud, K. A.; Dalal, N. S.; Gray, T. G.; Veige, A. S. *Inorg. Chem.* **2009**, *48*, 10901−10903. (j) Sarkar, S.; Carlson, A. R.; Veige, M. K.; Falkowski, J. M.; Abboud, K. A.; Veige, A. S. *J. Am. Chem. Soc.* **2008**, *130*, 1116−1117. (k) Sarkar, S.; Abboud, K. A.; Veige, A. S. *J. Am. Chem. Soc.* **2008**, *130*, 16128−16129. (l) Koller, J.; Sarkar, S.; Abboud, K. A.; Veige, A. S. *Organometallics* **2007**, *26*, 5438−5441.

(6) (a) Albrecht, M. *Chem. Rev.* **2010**, *110*, 576−623. (b) Ryabov, A. D. *Chem. Rev.* **1990**, *90*, 403−424.

(7) For specific examples of cyclometalation in tantalum chemistry, see: Rothwell, I. P. *Acc. Chem. Res.* **1988**, *21*, 153−159.

(8) $[Ar^{Tol_2}]I$ is synthesized by a method analogous to that used for $[Ar^{Ph_2}]I$. See Experimental Section.

(9) (a) Juvinall, G. L. *J. Am. Chem. Soc.* **1964**, *86*, 4202−4203. (b) Fowles, G. W. A.; Rice, D. A.; Wilkins, J. D. *J. Chem. Soc., Dalton Trans.* **1973**, 961−965. (c) Schrock, R. R.; Sharp, P. R. *J. Am. Chem. Soc.* **1978**, *100*, 2389−2399.

(10) This displacement is reproduced by density functional theory calculations (B3LYP using 6-31G** (C, H, Cl, and P) and LACVP (Ta) basis sets. (*Jaguar 7.5*; Schrödinger, LLC: New York, 2008) See Supporting Information for all geometry-optimized structures.

(11) For comparison, the mean displacement for structurally characterized tantalum−phenyl compounds listed in the Cambridge Structural Database (version 5.32) is 174.8°: Allen, F. H.; Kennard, O. 3D Search and Research using the Cambridge Structural Database. *Chem. Design Automation News* **1993**, *8* (1), 1 and 31−37.

(12) See, for example: (a) Steffey, B. D.; Fanwick, P. E.; Rothwell, I. P. *Polyhedron* **1990**, *9*, 963−968. (b) Kleinhenz, S.; Schubert, M.; Seppelt, K. *Chem. Ber. Recl.* **1997**, *130*, 903−906.

(13) (a) Zhu, Z.; Brynda, M.; Wright, R. J.; Fischer, R. C.; Merrill, W. A.; Rivard, E.; Wolf, R.; Fettinger, J. C.; Olmstead, M. M.; Power, P. P. *J. Am. Chem. Soc.* **2007**, *129*, 10847−10857. (b) Wang, Y.; Quillian, B.; Wannere, C. S.; Wei, P.; Schleyer, P. v. R.; Robinson, G. H. *Organometallics* **2007**, *26*, 3054−3056. (c) Quillian, B.; Wang, Y.; Wei, P.; Robinson, G. H. *New J. Chem.* **2008**, *32*, 774−776. (d) Ni, C.; Ellis, B. D.; Fettinger, J. C.; Long, G. J.; Power, P. P. *Chem. Commun.* **2008**, 1014−1016.

(14) Rabe, G. W.; Bérube, C. D.; Yap, G. P. A *Inorg. Chem.* **2001**, *40*, 2682−2685.

(15) Rabe, G. W.; Bérube, C. D.; Yap, G. P. A; Lam, K.-C.; Concolino, T. E.; Rheingold, A. L. *Inorg. Chem.* **2002**, *41*, 1446−1453.

(16) Niemeyer, M. *Acta Crystallogr.* **2001**, *E57*, m578−m580.

(17) Heckmann, G.; Niemeyer, M. *J. Am. Chem. Soc.* **2000**, *122*, 4227−4228.

(18) In-plane distortions of terphenyl ligands are also known. For example, $\{[Ar^{Pr^i_2}]Cr(\mu\text{-}Cl)\}_2$ has $Cr-C_{ipso}-C_{ortho}$ angles of 99.9° and 142.0°. See: Sutton, A. D.; Ngyuen, T.; Fettinger, J. C.; Olmstead, M. M.; Long, G. J.; Power, P. P. *Inorg. Chem.* **2007**, *46*, 4809−4814.

(19) For construction of an X_3 [*OCO*] pincer ligand on tantalum by elimination of methane, see: (a) Agapie, T.; Bercaw, J. E. *Organometallics* **2007**, *26*, 2957−2959. (b) Agapie, T.; Day, M. W.; Bercaw, J. E. *Organometallics* **2008**, *27*, 6123−6142.

(20) Low-temperature NMR spectroscopic evidence has been presented for the generation of selenium ate complexes derived from *m*-terphenyl derivatives. However, such complexes have neither been isolated nor structurally characterized by X-ray diffraction. See: (a) Reich, H. J.; Gudmundsson, B. O.; Dykstra, R. R. *J. Am. Chem. Soc.* **1992**, *114*, 7937−7938. (b) Reich, H. J.; Gudmundsson, B. O.; Green, D. P.; Bevan, M. J.; Reich, I. L. *Helv. Chim. Acta* **2002**, *85*, 3748−3772.

(21) The ability of PMe_3 to induce alkane elimination in Ta(V) compounds by α-H elimination is precedented. See, for example: (a) McLain, S. J.; Wood, C. D.; Messerle, L. W.; Schrock, R. R.; Hollander, F. J.; Youngs, W. J.; Churchill, M. R. *J. Am. Chem. Soc.* **1978**, *100*, 5962−5964. (b) Fellman, J. D.; Rupprecht, G. A.; Wood, C. D.; Schrock, R. R. *J. Am. Chem. Soc.* **1978**, *100*, 5964−5966. (c) Schrock, R. R. *Acc. Chem. Res.* **1979**, *12*, 98−104.

(22) Sattler, A.; Ruccolo, S.; Parkin, G. *Dalton Trans.* **2011**, *40*, 7777−7782.

(23) (a) Cloke, F. G. N.; Green, M. L. H. *J. Chem. Soc. Dalton Trans.* **1981**, 1983−1943. (b) Cloke, F. G. N.; Dix, A. N.; Green, J. C.; Perutz, R. N.; Seddon, E. A. *Organometallics* **1983**, *2*, 1150−1159. (c) Wigley, D. E.; Gray, S. D. In *Comprehensive Organometallic Chemistry II*; Abel, E. W., Stone, F. G. A., Wilkinson, G., Eds.; Elsevier: Oxford, 1995; Vol. *5*, Chapter 2, pp 57−153. (d) Mashima, K. In *Comprehensive Organometallic Chemistry III*; Crabtree, R. H., Mingos, D. M. P., Eds.; Elsevier: Oxford, 2006; Vol. *5*, Chapter 5.03, pp 101−200.

(24) For examples of structurally characterized tantalum complexes that feature other arenes, see: (a) Bruck, M. A.; Copenhaver, A. S.; Wigley, D. E. *J. Am. Chem. Soc.* **1987**, *109*, 6525−6527. (b) Wexler, P. A.; Wigley, D. E. *J. Chem. Soc., Chem. Commun.* **1989**, 664−665. (c) Arney, D. J.; Wexler, P. A.; Wigley, D. E. *Organometallics* **1990**, *9*, 1282−1289. (d) Wexler, P. A.; Wigley, D. E.; Koerner, J. B.; Albright, T. A. *Organometallics* **1991**, *10*, 2319−2327. (e) Arney, D. J.; Bruck, M. A.; Wigley, D. E. *Organometallics* **1991**, *10*, 3947−3949. (f) Smith, D. P.; Strickler, J. R.; Gray, S. D.; Bruck, M. A.; Holmes, R. S.; Wigley, D. E. *Organometallics* **1992**, *11*, 1275−1288. (g) Arney, D. S. J.; Fox, P. A.; Bruck, M. A.; Wigley, D. E. *Organometallics* **1997**, *16*, 3421−3430.

(25) Puckered arenes with folds in the opposite direction such that the two carbon atoms along the fold are farther from the metal are also known. See, for example: (a) Radonovich, L. J.; Koch, F. J.; Albright, T. A. *Inorg. Chem.* **1980**, *19*, 3373−3379. (b) Atwood, J. L.; Hunter, W. E.; Rogers, R. D.; Carmona-Guzman, E.; Wilkinson, G. *J. Chem. Soc., Dalton Trans.* **1979**, 1519−1523.

(26) For examples of arene complexes that feature puckered 1,4-cyclohexadienediyl geometries, see ref 24 and the following: (a) Churchill, M. R.; Chang, S. W.-Y. *J. Chem. Soc., Chem. Commun.* **1974**, 248−249. (b) Gardner, T. G.; Girolami, G. S. *Angew. Chem., Int. Ed.* **1988**, *27*, 1693−1695. (c) Hagadorn, J. R.; Arnold, J. *Angew. Chem., Int. Ed.* **1998**, *37*, 1729−1731. (d) Graham, T. W.; Kickham, J.; Courtenay, S.; Wei, P.; Stephan, D. W. *Organometallics* **2004**, *23*, 3309−3318. (e) Kissounko, D.; Epshteyn, A.; Fettinger, J. C.; Sita, L. R. *Organometallics* **2006**, *25*, 531−535. (f) Otten, E.; Meetsma, A.; Hessen, B. *J. Am. Chem. Soc.* **2007**, *129*, 10100−10101. (g) Kawaguchi, H.; Matsuo, T. *J. Am. Chem. Soc.* **2003**, *125*, 14254−14255.

(27) For other arene coordination modes, see: (a) Zhu, G.; Figueroa, J. S.; Parkin, G. *J. Am. Chem. Soc.* **2006**, *128*, 5452−5461. (b) Maslowsky, E. *J. Chem. Educ.* **1993**, *70*, 980−984.

(28) (a) Hall, M. B.; Fenske, R. F. *Inorg. Chem.* **1972**, *11*, 768. (b) Bursten, B. E.; Jensen, J. R.; Fenske, R. F. *J. Chem. Phys.* **1978**, *68*, 3320. (c) Manson, J.; Webster, C. E.; Pérez, L. M.; Hall, M. B. http://www.chem.tamu.edu/jimp2/index.html.

(29) The *z*-axis is defined as the $Ta-[C_6H_6]_{cent}$ axis, with the *x*- and *y*-axes lying in the TaC_3 and TaP_2 planes, respectively.

(30) (a) Redfield, D. A.; Cary, L. W.; Nelson, J. H. *Inorg. Chem.* **1975**, *14*, 50−59. (b) Nelson, J. H. *Concepts Magn. Reson.* **2002**, *14*, 19−78. (c) Redfield, D. A.; Nelson, J. H.; Cary, L. W. *Inorg. Nucl. Chem. Lett.* **1974**, *10*, 727−733.
(31) A similar five-line pattern is also observed in the $^{31}P\{^{1}H\}$ NMR spectrum of $[\kappa^3\text{-}Ar^{Tol'_2}]Ta(PMe_3)_2(^{13}CH_3)_2$.
(32) (a) Bishop, E. O.; Carey, P. R. *Mol. Phys.* **1970**, *18*, 845−850. (b) Ault, A. *J. Chem. Educ.* **1970**, *47*, 812−818. (c) Abraham, R. J.; Bernstein, H. J. *Can. J. Chem.* **1961**, *39*, 216−230.
(33) Bovey, F. A. *Nuclear Magnetic Resonance Spectroscopy*; Academic Press: New York, 1969.
(34) (a) Günther, H. *Angew. Chem., Int. Ed.* **1972**, *11*, 861−874. (b) McFarlane, W.; Rycroft, D. S. *J. Chem. Soc., Faraday Trans.* **1974**, 377−385.
(35) The derived value of $^{2}J_{CC} = 0$ for the $[Ta(^{13}CH_3)_2]$ moiety is consistent with the observation that there is no discernible $^{2}J_{CC}$ between the Ta−$^{13}CH_3$ groups of $[\kappa^3\text{-}Ar^{Tol'_2}]Ta(PMe_3)_2(^{13}CH_3)_2$ and the pincer carbon atoms.
(36) It is worth pointing out that, while the 1:4.7:11.4:4.7:1 intensity ratio is accord with the formulas presented in ref 33, another text (Becker, E. D. *High Resolution NMR. Theory and Chemical Applications*, 3rd ed.; Academic Press: New York, 2000) predicts an incorrect ratio because the intensities of transitions 5−12 of the general AA′XX′ pattern are listed as twice the correct values.
(37) (a) Baker, M. V.; Field, L. D. *Inorg. Chem.* **1987**, *26*, 2010−2011. (b) Goodfellow, R. J.; Taylor, B. F. *J. Chem. Soc., Dalton Trans.* **1974**, 1676−1684. (c) Verkade, J. G. *Coord. Chem. Rev.* **1972**, *9*, 1−106. (d) Pregosin, P. S.; Kunz, R. W. *NMR Basic Princ. Prog.* **1979**, *15*, 28−34.
(38) (a) Darensbourg, D. J. *J. Organomet. Chem.* **1981**, *209*, C37−C40. (b) Aime, S.; Osella, D. *J. Chem. Soc., Chem. Commun.* **1981**, 300−302. (c) Aime, S. *Inorg. Chim. Acta* **1982**, *62*, 51−56. (d) Hawkes, G. E.; Lian, L. Y.; Randall, E. W.; Sales, K. D.; Aime, S. *J. Chem. Soc., Dalton Trans.* **1985**, 225−227. (e) Tachikawa, M.; Richter, S. I.; Shapley, J. R. *J. Organomet. Chem.* **1977**, *128*, C9−C14. (f) Shapley, J. R.; Stuntz, G. F.; Churchill, M. R.; Hutchinson, J. P. *J. Chem. Soc., Chem. Commun.* **1979**, 219−220.
(39) (a) de Dios, A. C.; Jameson, C. J. *Annu. Rep. NMR Spectrosc.* **1994**, *29*, 1−69. (b) Hansen, P. E. *Annu. Rep. NMR Spectrosc.* **1983**, *15*, 105−234.
(40) For a related example, see: Gross, C. L.; Girolami, G. S. *Organometallics* **1996**, *15*, 5359−5367.
(41) For other examples, see: Hersh, W. H. *J. Chem. Educ.* **1997**, *74*, 1485−1488.
(42) The magnitude of $\Delta\delta_{PP}$ is comparable to the one-bond ^{13}C isotope effect on the ^{31}P chemical shift, $^{1}\Delta P(C)$, for other systems (0.022−0.025 ppm). See ref 40 and the following: (a) Maple, S. R.; Carson, J. E.; Allerhand, A. *J. Am. Chem. Soc.* **1989**, *111*, 7293−7295. (b) Aime, S.; Harris, R. K. *J. Magn. Reson.* **1974**, *13*, 236−238. (c) Buchner, W.; Ries, W.; Malisch, W. *Magn. Reson. Chem.* **1990**, *28*, 515−518.
(43) $^{3}J_{PC}$ was fixed to be zero because no $^{3}J_{PC}$ coupling is observed for $[\kappa^3\text{-}Ar^{Tol'_2}]Ta(PMe_3)_2MeCl$. Specifically, the chemical inequivalence of the phosphorus nuclei of $[\kappa^3\text{-}Ar^{Tol'_2}]Ta(PMe_3)_2MeCl$ is sufficiently large ($\Delta\delta_{PP}$ = 8.3 ppm) that the $^{13}C\{^{1}H\}$ signals for the PMe_3 ligands exhibit a first-order pattern, *i.e.*, two doublets with $^{1}J_{PC}$ coupling constants of 24 and 25 Hz.
(44) The appearance of the simulated spectra does not depend on the signs of either $^{2}J_{PP}$ or $^{1}J_{PC}$.
(45) This value of the secondary isotope effect was not refined but was assumed to be the same as that for $[\kappa^3\text{-}Ar^{Tol'_2}]Ta(PMe_3)_2Me_2$. Also see ref 42.
(46) Chamberlain, L. R.; Rothwell, I. P.; Huffman, J. C. *J. Am. Chem. Soc.* **1986**, *108*, 1502−1509.
(47) For related studies, see: Lockwood, M. A.; Clark, J. R.; Parkin, B. C.; Rothwell, I. P. *Chem. Commun.* **1996**, 1973−1974.
(48) Likewise, Bercaw has reported that elimination of toluene from $Cp^*_2Hf(CH_2Ph)_2$ to give the metallated complex $Cp^*_2Hf(\kappa^2\text{-}CH_2C_6H_4)$occurs *via* a sequence that primarily involves initial α-H abstraction to generate the benzylidene complex $Cp^*_2Hf{=}CHPh$ that undergoes 1,2-addition of a methyl C−H bond to give $Cp^*(\eta^5,\eta^1\text{-}C_5Me_4CH_2)HfCH_2Ph$, that subsequently isomerizes to $Cp^*_2Hf(\kappa^2\text{-}CH_2C_6H_4)$. See: Bulls, A. R.; Schaefer, W. P.; Serfas, M.; Bercaw, J. E. *Organometallics* **1987**, *6*, 1219−1226.
(49) Likewise, addition of PMe_3 to $[Ar^{Tol_2}]Ta(CD_3)_3Cl$ liberates CD_3H and forms $[\kappa^3\text{-}Ar^{Tol'_2}]Ta(PMe_3)_2(CD_3)Cl$.
(50) In addition to CD_4, the α-H abstraction pathway would also result in the formation of other methane isotopologues.
(51) (a) McNally, J. P.; Leong, V. S.; Cooper, N. J. In *Experimental Organometallic Chemistry*; Wayda, A. L., Darensbourg, M. Y., Eds.; American Chemical Society: Washington, DC, 1987; Chapter 2, pp 6−23. (b) Burger, B. J.; Bercaw, J. E. In *Experimental Organometallic Chemistry*; Wayda, A. L., Darensbourg, M. Y., Eds.; American Chemical Society: Washington, DC, 1987; Chapter 4, pp 79−98. (c) Shriver, D. F.; Drezdzon, M. A. *The Manipulation of Air-Sensitive Compounds*, 2nd ed.; Wiley-Interscience: New York, 1986.
(52) Gottlieb, H. E.; Kotlyar, V.; Nudelman, A. *J. Org. Chem.* **1997**, *62*, 7512−7515.
(53) Nelson, J. H. *Nuclear Magnetic Resonance Spectroscopy*; Prentice Hall: Englewood Cliffs, NJ, 2003; p 79.
(54) Pray, A. R. *Inorg. Synth.* **1957**, *5*, 153−156.
(55) (a) Sheldrick, G. M. *SHELXTL*, An Integrated System for Solving, Refining and Displaying Crystal Structures from Diffraction Data; University of Göttingen: Göttingen, Federal Republic of Germany, 1981. (b) Sheldrick, G. M. *Acta Crystallogr.* **2008**, *A64*, 112−122.
(56) *Jaguar 7.5*; Schrödinger, LLC: New York, NY, 2008.
(57) (a) Becke, A. D. *J. Chem. Phys.* **1993**, *98*, 5648−5652. (b) Becke, A. D. *Phys. Rev. A* **1988**, *38*, 3098−3100. (c) Lee, C. T.; Yang, W.; Parr, R. G. *Phys. Rev. B* **1988**, *37*, 785−789. (d) Vosko, S. H.; Wilk, L.; Nusair, M. *Can. J. Phys.* **1980**, *58*, 1200−1211. (e) Slater, J. C. *Quantum Theory of Molecules and Solids. Vol. 4: The Self-Consistent Field for Molecules and Solids*; McGraw-Hill: New York, 1974.
(58) (a) Hay, P. J.; Wadt, W. R. *J. Chem. Phys.* **1985**, *82*, 270−283. (b) Wadt, W. R.; Hay, P. J. *J. Chem. Phys.* **1985**, *82*, 284−298. (c) Hay, P. J.; Wadt, W. R. *J. Chem. Phys.* **1985**, *82*, 299−310.
(59) Lichtenberger, D. L. *MOPLOT*, version 2.0; Department of Chemistry, University of Arizona: Tuscon, AZ, June 1993.
(60) (a) Wright, R. J.; Steiner, J.; Beaini, S.; Power, P. P. *Inorg. Chim. Acta* **2006**, *359*, 1939−1946. (b) Saednya, A.; Hart, H. *Synthesis* **1996**, 1455−1458.